AD_____

Award Number: W81XWH-06-1-0107

TITLE: The Influence of Physical Forces on Progenitor Cell Migration, Proliferation and Differentiation in Fracture Repair

PRINCIPAL INVESTIGATOR:

Steven A. Goldstein, PhD
Kurt Hankenson, DVM, PhD
Michael Kilbourn, PhD

CONTRACTING ORGANIZATION:

The University of Michigan
Ann Arbor, MI 48109-1274

REPORT DATE: November 2009

TYPE OF REPORT: Final

PREPARED FOR: U.S. Army Medical Research and Materiel Command
Fort Detrick, Maryland 21702-5012

DISTRIBUTION STATEMENT:

X Approved for public release; distribution unlimited

REPORT DOCUMENTATION PAGE

Form Approved
OMB No. 0704-0188

1. REPORT DATE *(DD-MM-YYYY)*	**2. REPORT TYPE**	**3. DATES COVERED** *(From - To)*
01-11-2009	Final	11/1/05 – 10/31/09

4. TITLE AND SUBTITLE
The Influence of Physical Forces on Progenitor Cell Migration, Proliferation and Differentiation in Fracture Repair

5a. CONTRACT NUMBER

5b. GRANT NUMBER
W81XWH-06-1-1017

5c. PROGRAM ELEMENT NUMBER

6. AUTHOR(S)
Steven A. Goldstein, PhD

Kurt Hankenson, DVM, PhD

Michael Kilbourn, PhD

5d. PROJECT NUMBER

5e. TASK NUMBER

5f. WORK UNIT NUMBER

7. PERFORMING ORGANIZATION NAME(S) AND ADDRESS(ES)
The University of Michigan

Ann Arbor, MI 48109-1274

8. PERFORMING ORGANIZATION REPORT NUMBER

9. SPONSORING / MONITORING AGENCY NAME(S) AND ADDRESS(ES)
U.S. Army Medical Research and Materiel Command
Fort Detrick, MD 21702-5012

10. SPONSOR/MONITOR'S ACRONYM(S)

11. SPONSOR/MONITOR'S REPORT NUMBER(S)

12. DISTRIBUTION / AVAILABILITY STATEMENT
Approved for public release; distribution unlimited

13. SUPPLEMENTARY NOTES

14. ABSTRACT
The goal of this program is to investigate the influence of controlled mechanical stimulation on the behavior of progenitor cells in an effort to develop strategies to significantly enhance the rate and quality of fracture repair in long bone. All of the proposed studies in the program were completed. The results demonstrate that the application of load increases the callus volume, bone mineral density and biomechanical properties. More importantly, the data demonstrates a substantial independence on the time of load application. Load stimulation can positively influence fracture repair when applied at 10 or 24 days after fracture, while early application (during granulation tissue formation) may be detrimental to tissue regeneration. We also demonstrated that systemically introduced progenitor cells play an indirect role on the repair and identified a variety of factors that may be associated with repair cell recruitment. Surprisingly, the introduction of cells locally into the fracture site were detrimental to the repair process and unaffected by load. The results provide a rationale for new strategies for enhancing fracture repair.

15. SUBJECT TERMS
Long Bones, Fracture Healing, Regeneration, MSC's

16. SECURITY CLASSIFICATION OF:			**17. LIMITATION OF ABSTRACT**	**18. NUMBER OF PAGES**	**19a. NAME OF RESPONSIBLE PERSON**
a. REPORT	**b. ABSTRACT**	**c. THIS PAGE**			USAMRMC
U	U	U	UU	62	**19b. TELEPHONE NUMBER** *(include area code)*

Standard Form 298 (Rev. 8-98)
Prescribed by ANSI Std. Z39.18

Table of Contents

Page

Introduction

The goal of this program is to investigate the influence of controlled mechanical stimulation on the behavior of progenitor cells in an effort to develop strategies to significantly enhance the rate and quality of fracture repair in long bones. In support of these goals, we tested the global hypothesis that the migration, proliferation and differentiation of systemically or locally delivered MSCs is temporarily dependent on local mechanical conditions within the regenerate tissues.

Body

The final progress report of this research program is described below, as a function of the statements of work that were approved by the USAMRMC. The statement of work was proposed as follows:

1. Acquisition of transgenic GFP rats and establishment of a small colony for cell donation. This will be accomplished in the first eight months of the study.

2. Extraction, isolation and expansion of MSC from transgenic GFP rats to establish baseline of GFP signal in culture. This will occur during year 1.

3. Delivery of MSCs from GFP rats into wild type rats after treatment with F^{18}. This will be a dosing and cell viability study using microPET imaging and will be accomplished during year 1.

4. Fabrication of the required external fixation devices, associated pins and surgical guides will be performed during years 1 through 3.

5. Implementation of the first primary experiment: 108 rats with bilateral femoral 2mm defects and fixation will be entered into the study to evaluate the effect of load and systemic cell delivery on cell migration, using microPET scanning. Animals will be entered in year 1 through year 2.

6. The evaluation of the effect of delivery and mechanical stimulation on bone regeneration using histologic, micro-imaging and biomechanical assays will be performed in years 1 through 2.5.

7. 144 animals will be entered into the second primary experiment to evaluate the effect of local cell delivery and mechanical stimulation during years 2.5 through 3.5.

8. Complete analysis of the combined effects of local or systemic cell delivery with mechanical stimulation will be completed during years 3.5 through 4.

All of the tasks and objectives have been completed in this study. Since this is a final report, a brief summary of the progress for years 1 through 3 will be given, as well as, a more specific report of results for the final year (year 4).

Brief review and summary of progress from years 1 to 3 as referenced to tasks and objectives from original proposal.

1. Acquisition of transgenic GFP rats and establishment of a small colony for cell donation. A colony of GFP rats was established based on founders acquired from Japan. These animals served well as donors of the transplanted MSCs. As a result, using both fluorescent microscopy and immunohistochemistry, we were able to identify the donor cells or their progeny in the histologic samples from the study. The colony has now been transferred to other investigators, who's studies will benefit from these animals.

2. Extraction, isolation and expansion of MSC from transgenic GFP rats to establish baseline of GFP signal in culture. This was established and demonstrated that the cells from the donor colony were expressing GFP protein.

3. Delivery of MSCs from GFP rats into wild type rats after treatment with F^{18}. This will be a dosing and cell viability study using microPET. As noted in our earlier progress reports, the studies demonstrated that the rate of systemic cell migration was not consistent with the use of MicroPET analysis and we altered our methods to utilize SPECT scanning with Indium ^{111} labeling of the MSCs.

4. Fabrication of the required external fixation devices, associated pins and surgical guides. We successfully designed, fabricated and utilized the external fixation system and associated unique servo-controlled loading system. This system allowed us to successfully complete all the in vivo studies.

5. Implementation of the first primary experiment: 108 rats with bilateral femoral 2mm defects and fixation will be entered into the study to evaluate the effect of load and systemic cell delivery on cell migration, using microPET scanning.

6. The evaluation of the effect of delivery and mechanical stimulation on bone regeneration using histologic, micro-imaging and biomechanical assays.

All 108 animals completed the study as designated by the original experimental design (except that the imaging studies were performed on a separate group of animals). To review, the experimental design is summarized in table 1. Note the specific variations in load initiation time (post-surgery) and sacrifice time.

Group (total # animals)	Surgery Day	Loading initiation and cell delivery	Euthanasia Day 10 (# animals)	Euthanasia Day 24 (# animals)	Euthanasia Day 48 (# animals)
A (36)	0	0	(12)	(12)	(12)
B (36)	0	3	(12)	(12)	(12)
C (24)	0	10	-	(12)	(12)
D 12)	0	24	-	-	(12)
108 total animals					

Loading was performed using a computer controlled axial loading system and included a sinusoidal waveform at 0.5 Hz. for 17 minutes for a total of 510 cycles at 8% global strain in tension and compression.

All animals had cell injections systemically by tail vein injection. Importantly, since our early analysis suggested a significant effect of load on progenitor cell migration and homing, **we added a new, modest experiment** to begin a search for specific biologic factors that might be responsible for the "homing" response. This experiment included the following:
12 rats were divided into 4 groups:

Group 1: bilateral fixators/osteotomies, loaded on days 3-7, euthanized day 7.
Group 2: unilateral fixator/osteotomy, no load, euthanized on day 7
Group 3: bilateral fixators/osteotomies, loaded on days 24-28, euthanized day 28
Group 4: unilateral fixator/osteotomy, no load, euthanized on day 28

Immediately after each animal was euthanized, the callus tissue was removed under sterile conditions. The legs of each animal were shaved, the femora were exposed and harvested, and the fracture calluses were removed from the osteotomy using a scalpel blade. After each callus was removed, it was immediately placed in an RNase-free microfuge tube and snap frozen in liquid nitrogen. The harvested tissues were then stored at -80°C until they were processed for RNA extraction. Using standard procedures, the RNA was extracted and then processed for RT-PCR Array analysis. The concentration of RNA for each sample was determined by spectrometer. All of the samples except one, which had a lower concentration, were diluted to a concentration of 126 ng/µl. Samples were examined on an Agilent 2100 bioanalyzer (Agilent Technologies, Santa Clara, California) to determine the integrity of the RNA. Two, 5µl amounts of each sample were alloquated for analysis, and all experiments were performed in duplicate. An RT2 ProfilerTM PCR Array System (all components from SABiosciences, Frederick, MD) was used for PCR analysis. The RNA in the 5µl samples was converted to cDNA using the RT2 First Strand Kit, and the experimental cocktail for RT-PCR was created using the RT2 qPCR master mix. A 384-well, custom PCR array was used to determine the expression of selected genes. Each array contained four sets of a panel of 84 genes of interest (See Table 1 and Table 2), five housekeeping genes, and three RNA and PCR quality controls. The genes of interest were selected through a literature search and chosen due to evidence that they are involved in the migration of

mesenchymal stem cells (1-27). The specific genes selected are illustrated in tables 2 and 3.

Table 2,3: Gene candidates selected for PCR array

Symbol	Description
Cxcl12	Chemokine (C-X-C motif) ligand 12
Il1a	Interleukin 1 alpha
Il1b	Interleukin 1 beta
Il6	Interleukin 6
Tnf	Tumor necrosis factor
Tgfb1	Transforming growth factor, beta 1
Tgfb2	Transforming growth factor, beta 2
Tgfb3	Transforming growth factor, beta 3
Pdgfa	Platelet derived growth factor, alpha
Pdgfb	Platelet derived growth factor, beta
Bmp1	Bone morphogenetic protein 1
Bmp2	Bone morphogenetic protein 2
Bmp3	Bone morphogenetic protein 3
Bmp4	Bone morphogenetic protein 4
Bmp5_predicted	Bone morphogenetic protein 5 (predicted)
Bmp6	Bone morphogenetic protein 6
Bmp7	Bone morphogenetic protein 7
Cxcl1	Chemokine (C-X-C motif) ligand 1
Gdf5	Growth differentiation factor 5
Gdf8	Growth differentiation factor 8
Fn1	Fibronectin 1
Vtn	Vitronectin
Col1a1	Procollagen, type 1, alpha 1
Angpt1	Angiopoietin 1
Angpt2	Angiopoietin 2
Vegfa	Vascular endothelial growth factor A
Vegfb	Vascular endothelial growth factor B
Vegfc	Vascular endothelial growth factor C
Igf1	Insulin-like growth factor 1
Cd44	CD44 antigen

Symbol	Description
Ihh	Indian hedgehog homolog, (Drosophila)
Bglap2	Bone gamma-carboxyglutamate protein 2
Igf2	Insulin-like growth factor 2
Fgf1	Fibroblast growth factor 1
Fgf2	Fibroblast growth factor 2
Fgf3	Fibroblast growth factor 3
Fgf4	Fibroblast growth factor 4
Fgf5	Fibroblast growth factor 5
Mmp2	Matrix metallopeptidase 2
Mmp7	Matrix metallopeptidase 7
Mmp8	Matrix metallopeptidase 8
Cx3cl1	Chemokine (C-X3-C motif) ligand 1
Cxcl16	Similar to chemokine (C-X-C motif) ligand 16
Mip1	Myocardial ischemic preconditioning 1
Egf	Epidermal growth factor
Hbegf	Heparin-binding EGF-like growth factor
Tgfa	Transforming growth factor alpha
Hgf	Hepatocyte growth factor
F2	Coagulation factor II
Ccl2	Chemokine (C-C motif) ligand 2
Ccl5	Chemokine (C-C motif) ligand 5
Ccl22	Chemokine (C-C motif) ligand 22
Lif	Leukemia inhibitory factor
Ntf3	Neurotrophin 3
Pgf	Placental growth factor
Cxcl10	Chemokine (C-X-C motif) ligand 10
Csf2	Colony stimulating factor 2 (gran-macrophage)
Csf3	Colony stimulating factor 3 (granulocyte)
Ibsp	Integrin binding bone sialoprotein
Flt1	FMS-like tyrosine kinase 1

Bmpr1a	Bone morphogenetic protein receptor, type 1A
Bmpr1b	Bone morphogenetic protein receptor, type 1B (mapped)
Bmpr2	Bone morphogenic protein receptor, type 2
Igf1r	Insulin-like growth factor 1 receptor
Igf2r	Insulin-like growth factor 2 receptor
Pdgfra	Platelet derived growth factor receptor, alpha polypeptide
Pdgfrb	Platelet derived growth factor receptor, beta polypeptide
Kdr	Kinase insert domain protein receptor
Ccr1	Chemokine (C-C motif) receptor 1
Ccr2	Chemokine (C-C motif) receptor 2
Ccr4	Chemokine (C-C motif) receptor 4
Ccr7	Chemokine (C-C motif) receptor 7
Il8rb	Interleukin 8 receptor, beta
Cxcr3	Chemokine (C-X-C motif) receptor 3
Cxcr4	Chemokine (C-X-C motif) receptor 4
Cxcr6	Chemokine (C-X-C motif) receptor 6
Fgfr1	Fibroblast growth factor receptor 1
Fgfr2	Fibroblast growth factor receptor 2
Fgfr3	Fibroblast growth factor receptor 3

Results

A. Results for primary experiment in Phase I studies (MicroCT, biomechanical tests)

The ratio of the stimulated to the control limbs shows decreases in all measures of mineralization for the groups displaced three days post-operatively. This decrease was as high as 19% in the BVF for animals euthanized at day 48. (Figures 1,2) All other groups showed an increase in mineralization in the stimulated fractures when compared to the unloaded controls. For rats that were sacrificed ten days after surgery (groups A10 and B10), there is a significant difference in the interaction of treatment and the timing of displacement. In those animals, displacement decreased both the callus volume and BMC in fractures stimulated starting on day three (group B10), while stimulation increased the same measurements in fractures stimulated immediately after surgery (group A10). The decrease between the loaded and control limbs within group B10 is significant for the callus volume, and the BMC within group A10 trends toward an increase (p=0.074).

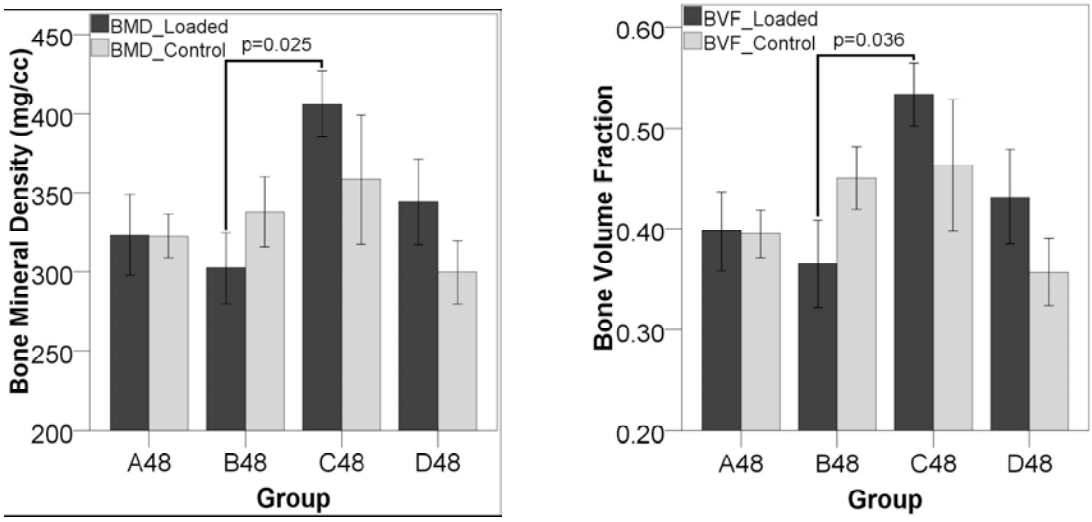

Figures 1,2: BMD and BVF are significantly higher in Group C (day ten displacement) versus Group B (day three displacement) 48 days after surgery. In the later stages of healing, the mineral content is higher on the displaced side in the animals loaded ten days post-operatively than those at other stimulation time points. This reached a significant increase over the defects displaced three days post-op, since the mineral levels in those gaps were slightly depressed compared to the other groups.

When fractures are analyzed 24 days post-operatively, there is a strong trend for differences across all of the loaded limbs in BMC (p=0.055) and BMD (p=0.059). Looking for differences between individual groups reveals that there is less mineralized tissue in the displaced fracture gaps of the animals stimulated on day three versus the animals stimulated on either day zero or day ten. This difference reached significance for BMD between groups B (stimulation day 3) and C (stimulation day 10) (Figure 1). At day 48, there is a significant difference in the BMD (p=0.045) and BVF (p=0.049) across all the stimulated limbs (Figure 3). Individually, there is a difference between the group displaced three days

post surgery (group B48) and the group displaced ten days post surgery (group C48), with the loaded defects from C48 having more mineral than those in B48. Along with the increased mineral content in the fractures stimulated ten days post-op, there is a significant decrease in cartilage in the healing defect for that group. The loaded limbs in group C48 have significantly less cartilage than their contralateral controls (p=0.045), while the loaded limbs in group A48 have more cartilage than there contralateral controls (p=0.037). There is also a difference in cartilage area between limbs stimulated at day ten and limbs that were stimulated at day zero (p=0.031) or day three (p=0.015). Stimulation starting at day three (group B10) induced more cartilage formation by day ten than did stimulation immediately after surgery (group A10). It also shows that the control limbs in the B10 group have a larger cartilage area than the controls from group A10 suggesting a possible systemic effect.

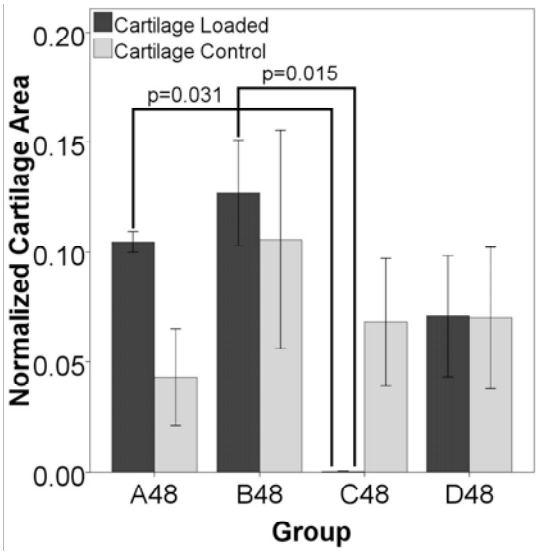

Figure 3:After 48 days, there is cartilage remaining in all groups, both stimulated and control, except for the gaps stimulated ten days after surgery (group C48). The differences were significant between the displaced limbs of A48 and B48 in comparison to C48. There is also a significant difference between the displaced and contralateral control in group C48 (p=0.045), with the displaced side containing significantly less cartilage than the control. There is also more cartilage in the displaced side in group A48 when compared to the contralateral control (p=0.037).

In animals euthanized on day 48, there is a significantly larger percentage of bone in the fracture gaps as measured by histology on both the loaded and control sides for the animals loaded starting on day ten (group C48) than for any other group.

B. Tracking of Progenitor Cells

As noted in earlier progress reports, we used SPECT imaging of Indium ^{111} labeled cells to track whether the progenitor cells would preferentially migrate to sites of repair and in particular to sites of mechanical stimulation.

A detectable number of MSCs are delivered to both femora after a systemic injection of cells as measured by planar gamma imaging. A high number of cells also remain in the visceral organs, especially the lungs, spleen, and liver. Over the course of the three days, the cells began to migrate towards the lower extremities. This pattern was not seen when indium^{111} was injected without first being incubated with MSCs. In the femora, immediately after injection (displacement day one) there is a strong trend (p=0.0586) toward more activity in the stimulated femora in comparison to the controls regardless of when displacement was initiated (Figure 4). On day one, there is significantly more activity in the stimulated limbs of the rats displaced on day three (group B) and a trend for more

activity in the rats stimulated on day 24 (group D). On the second day of loading, the timing of displacement administration with respect to the systemic injection of cells had a significant bearing on the migration of the MSCs, regardless of side (p=0.0079 (Figure 5). The group in which displacement did not start until three days after injection (group E) had significantly less activity on both the stimulated and control sides as compared to groups B (displacement day three) and D (displacement day ten) and a trend toward less activity when compared to group A (displacement day zero). By the third day of scanning, there were no differences within or between groups.

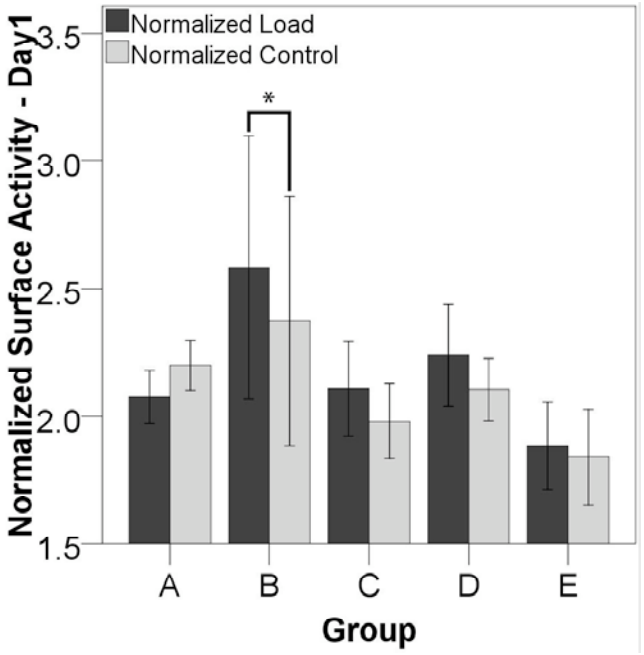

Figure 4: The normalized surface activity of the femora after the first application of axial displacement. The displaced limbs in the rats stimulated starting three days after surgery (group B) showed an increase in radioactivity when compared to the unloaded controls (*p<0.05). There was also a trend for an increase in the displaced limbs of the rats stimulated 24 days after surgery (group D) (p=0.0818).

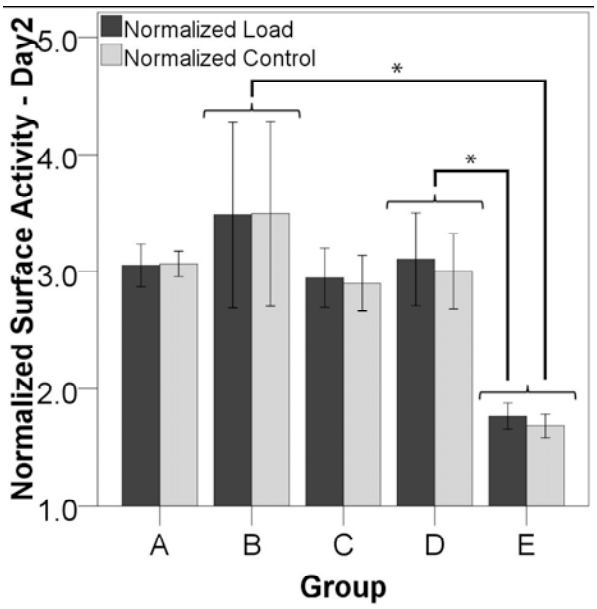

Figure 5: The group that was injected with MSCs after three bouts of displacement (group E) shows less activity in both limbs than in any other group. There was a significant difference for both the stimulated and control values across all groups. The effect of load initiation was also significant for groups B and D when compared to group E (there was a trend between groups A and E). This indicates that a smaller proportion of injected cells are available to both femora when the delivery of cells is delayed until axial displacement has already begun. (*p<0.05)

C. Immunohistochemistry analysis of GFP donor cell

In an effort to track the fate of the donor cells, we performed immunohistochemistry of the introduced cells. Since the cells were extracted from the GFP transgenic rats, their fate or the fate of their daughter cells could be tracked.

IHC shows that even though there is a small number of exogenous MSCs present throughout the healing process, the largest population of cells does not appear until 48 days after surgery. At that time, MSCs are detected in large populations throughout the marrow in the medullary canal (Figure 6) and the marrow spaces within the periosteal callus (Figure 7). This is true for all of the groups euthanized on day 48 except for the group stimulated ten days post-op (group C). It also appears that stimulation slightly increases the number of cells in the fractured limb, as the scores for the stimulated limbs were slightly higher than the control limbs at most time points. These results likely suggest that the role taken by the cells is dominantly to express factors that help to condition the wound site as opposed to differentiating into matrix producing cells.

D. PCR array results

In animals that underwent axial displacement starting three days after surgery and then were euthanized on day seven, IGF-2, IGF-2 receptor, and Col1a1 were up-regulated in the loaded fracture gap versus the contralateral control gap. HGF and angiopoietin-1 were down-regulated in the loaded callus tissue when compared to the contralateral control. For animals that were stimulated starting on day 24 and euthanized on day 28, CXCL-10 (IP-10), BMP-6, Bglap-2 (BGPR), EGF, and Ihh were all up-regulated in the displaced fracture tissue versus the contralateral control. Several genes were also down-regulated in the stimulated callus in comparison to the control including IL-8 receptor beta, MMP-8, CX3CR-1, IL-6, and CSF-3. To test for effects that the displaced gap may be having on the distant, control fracture, the control fracture tissue from animals that had bilateral osteotomies was compared to the fracture gaps from animals that only had one, unstimulated osteotomy. HGF, CCL22 (MDC), and TNF-α were up-regulated in tissue from control fractures in bilateral rats stimulated starting day three in comparison to the fractures in the unilateral model. IBSP, GDF-5, Col1a1, Ihh, MMP-2, and Fn-1 were all downregulated in those animals. For animals euthanized on day 28, FGF-4 and CX3CR-1 were up-regulated in control fractures from the bilateral rats versus the fracture tissue from the rats with only one osteotomy. Ihh, BMP-6, CXCL-1, IBSP, FGF-3, CXCL-10 (IP-10), GDF-5, and CSF-3 were all down-regulated in the same comparison.

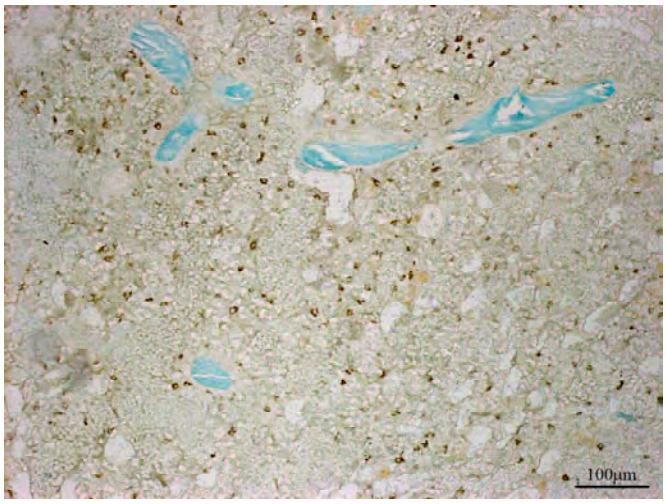

Figure 6: GFP positive cells in the marrow 48 days after surgery (brown stained cells) . At all of the time points there was evidence of some GFP positive staining, but it was not until day 48 that there were large populations of GFP positive cells in the marrow spaces. Cells were also present in other locations (cortices and pin sites), but the most consistent location for the MSC populations was in the medullary marrow and the marrow within the periosteal callus.

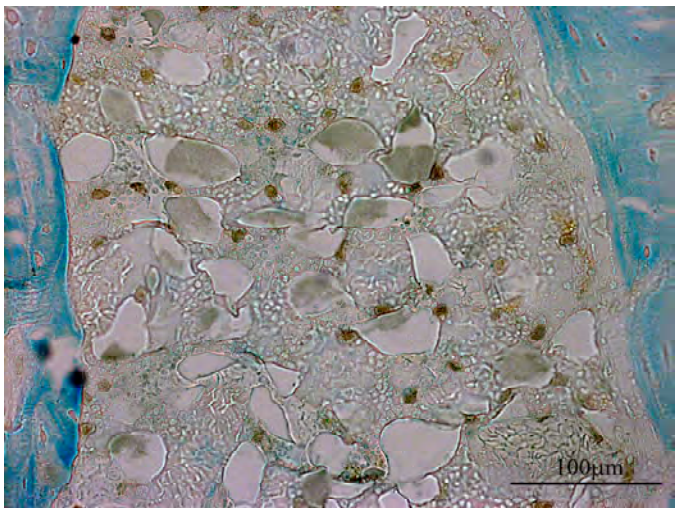

Figure 7: GFP positive cells in the periosteal callus (brown stained). The injected MSCs populated any area that consisted of marrow spaces. The areas in between the original cortex and the hard callus shell that formed from a periosteal response consist of marrow tissue. The injected MSCs were often found in these areas. The above image is of cells in the periosteal callus.

Discussion

The observation that the application of displacement on the animals soon after surgery decreased mineralization and mechanical properties in relation to the animals that had displacement starting on day ten suggests that axial mechanical stimulation may not be beneficial when it is started during the initial response to fracture. Vascular supply is an important factor in determining the success of healing, and it has been suggested that it may be necessary to allow neovascularization to progress at the site of repair before mechanical load is applied (28, 29). If motion is allowed too soon at the fracture site, the capillaries needed to support osseous tissues are constantly ruptured, and fibrocartilage formation is promoted since it requires less vascularization (30). Therefore, it may be beneficial to the overall healing outcome to delay initiation of loading until new vessels have had a chance to form (31).

The results also suggest that it may be beneficial to start fracture stimulation after the inflammatory stage, when some soft tissues have had a chance to form. After the initial inflammatory response, cells that may be responsive to load, such as chondrocytes (32,33), have an opportunity to populate the fracture site. A beneficial response to chondrocyte

loading in fracture healing has been shown. Scaffolds seeded with chondrocytes that were implanted in the femora of rabbits and then were compressively loaded had a higher bone volume fraction than the unloaded controls (34), showing that the application of a stimulus to a chondrocyte population may encourage bone formation at the site of repair.

A controlled, axial stimulation has a definitive effect on fracture healing, and the timing of the application of the displacement differentially effects callus morphology and mechanical properties. Stimulation early in the repair process was not beneficial to fracture healing, but when the displacement was applied starting ten days after injury it increased mineralization, accelerated callus remodeling, and increased torsional mechanical properties in comparison to other groups. The beneficial effect was seen on both the experimental and the contralateral control defects, indicating that there may be a systemic effect from the applied stimulus.

Despite the fact that the cell number initially prevents the cells from moving freely through the circulation, some of the cells do find their way to the injured limbs. They do not localize to the injury directly, but instead the activity seems to encompass the entire femur. This may be due to the fact that the surgical procedure involves the placement of four bicortical pins to stabilize the fracture. These pins may act as additional sites of injury that encourage the cells to populate the region around the entire femur as opposed to localizing to the osteotomy. The planar gamma images also show a transient difference in the radioactivity detected between different groups. On the first day of axial displacement, the stimulation increases the activity in the loaded limbs versus the unstimulated controls. That difference disappears by day two, when no differences between the two sides are observed. On day two though, there is a difference between all of the groups that underwent axial displacement immediately after cell injection and the animals in which cell injection was delayed until the fourth day of stimulation (group E). This may suggest a transient systemic effect of load timing in relation to when the cells are delivered, as activity on both sides of the late delivered cell group showed a decrease. This effect could be due to many factors. The extra sessions of axial displacement could have triggered the systemic release of antimigratory factors (or hindered the expression of migratory factors). Damage that could be induced by displacement could have accumulated over the course of the first three days and caused an adverse response. All of the radioactivity differences appear to be transient though, as there were no differences between any group by day three. The inability to detect differences by that time point may also be due to a decline in sensitivity, as the half-life of indium^{111} is about three days, which would reduce the overall signal that can be detected.

The sections stained for GFP through IHC confirmed that cells are able to migrate to the femora. It also showed that the injected MSCs were, in most cases, able to establish a population in the marrow by day 48. The exogenous MSCs were found in other locations other than marrow compartments, but it seems that the most consistent populations were found in the marrow. This is probably because the marrow and the cambium layer of the periosteum are considered primary stem cell niches (35) and so it is natural for the cells to engraft there as opposed to other locations. This is consistent with other studies that have found exogenous MSCs in the bone marrow for long periods after a systemic injection (36), and do not appear in large numbers in the first few weeks after delivery (37). Most of these other studies though involve pretransplant conditioning like irradiation of the host animal (38), while few have been able to show long-term engraftment after bone marrow transplants without conditioning.

Final studies: Phase II studies and results

The phase II studies were designed to evaluate the influence of mechanical stimulation and local implantation of progenitor cells. The task associated with Phase II was as follows:

7. 108 animals were entered into the second primary experiment to evaluate the effect of local cell delivery and mechanical stimulation.

In order to perform the Phase II studies, we needed to develop the delivery matrices for the cells. As described in the original proposal, the matrix utilized was demineralized bone matrix (DBM). As a result, we developed the protocols for producing the DBM as well as tested the cell viability in the delivery scaffold. Prior to initiating the full study we needed to perform several preliminary studies. The specific accomplishments are described below.

a. Protocols for producing DBM from Sprague Dawley rats was developed and tested.
b. A preliminary study was performed, in vitro, to ensure that the GFP MSCs would remain viable in the DBX. The results demonstrated that the cells were viable and the delivery technique was valid.
c. We developed and validated a technique for reproducibly creating constructs consisting of DBM and 1,000,000 cells in a 2mm. X 3mm. cylindrical geometry that could be delivered into the femoral defects.
d. We mass produced sufficient DBM scaffolds to complete the entire Phase II study and had them sterilized by gamma irradiation. All were maintained in sterile containers, ready for mixing with the cell constructs prior to surgical insertion.

Following these preliminary studies all 108 animals were entered and completed the Phase II studies. The experimental design was very similar to Phase I, except that the cells were delivered locally by incorporating them into the matrix as described above. The detailed design is illustrated below.

Phase II study design

Group (total # animals)	Surgery Day and local delivery of cells	Loading initiation	Euthanasia Day 10 (# animals)	Euthanasia Day 24 (# animals)	Euthanasia Day 48 (# animals)
A (36)	0	0	(12)	(12)	(12)
B (36)	0	3	(12)	(12)	(12)
C (24)	0	10	-	(12)	(12)
D 12)	0	24	-	-	(12)
108 total animals					

Results of Phase II

Overall, the results of Phase II were very disappointing, although they may be very important as the field continues to investigate techniques for enhancing bone regeneration and repair. **Essentially, the delivery of the local cell populations into the fracture gap delayed and perhaps even prevented effective healing from occurring**. We found this surprising, but perhaps there are several explanations or theories for these findings. Prior to discussing these results, a brief summary of some of the data is provided below.

Microcomputed Tomography

Review of the MicroCT data was perhaps the most informative method of demonstrating the results of these studies. In general, the same procedures were used for the analysis, as in phase I. Briefly, immediately after sacrifice, both femora were excised and the surrounding soft tissue was removed without disturbing the callus around the fracture site. A temporary fixator was then placed adjacent to the existing fixator to facilitate the removal of the original fixator and central pins. The original fixator and the two central pins were removed in order to both fit the specimen into the scanner and to eliminate metal from the volume to be scanned to reduce artifacts. Bones were scanned via *ex-vivo* micro-CT (GE Healthcare Pre-Clinical Imaging, London, ON) at a voxel size of 18 microns. After scanning, a region of interest was created encompassing the 2mm osteotomy site and any remaining cortical bone was subtracted from the region. The lateral borders of the region of interest were defined by visible mineralization on the outermost boundary of the callus. After defining the region and applying a threshold to distinguish mineralized from non-mineralized tissue we determined bone mineral content (BMC), bone mineral density (BMD), the tissue mineral content (TMC) and the tissue mineral density (TMD). Finally, the bone volume fraction (BVF) of the callus was determined.

Bone Mineral Density (BMD)

The analysis includes data from groups euthanized after10 days post op. The first and most obvious findings were that very little healing was seen in the specimens, which made segmentation of the data for analysis difficult. As illustrated, there was an increase in mineralization from 24 to 48 days, but no effect of load. It should also be noted that these overall values are consistent with poor healing.

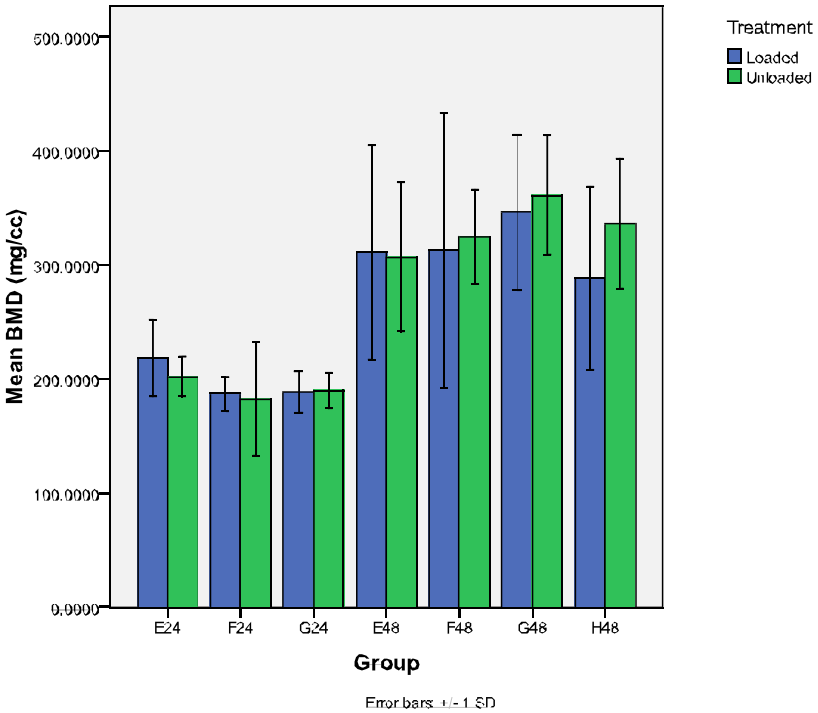

The same results were essentially found for tissue mineral content, callus volume, and bone volume fraction; no difference as a result of loading and large standard deviations.

Tissue Mineral Content (TMC) ***Callus Volume***

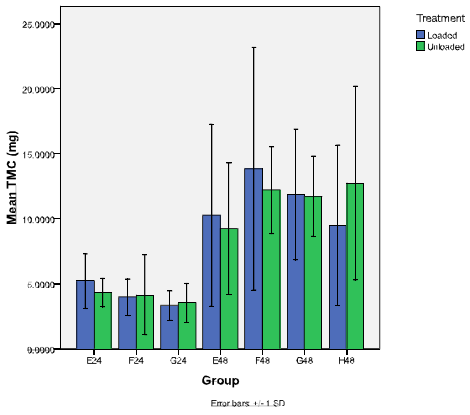

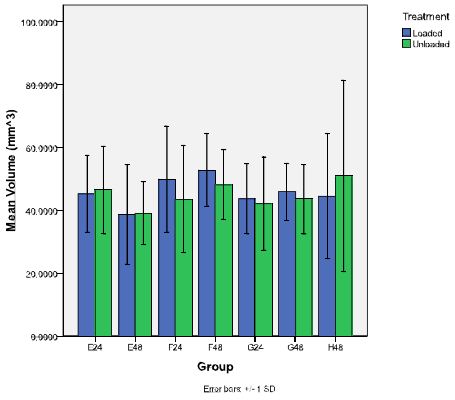

Bone Volume Fraction (BVF)

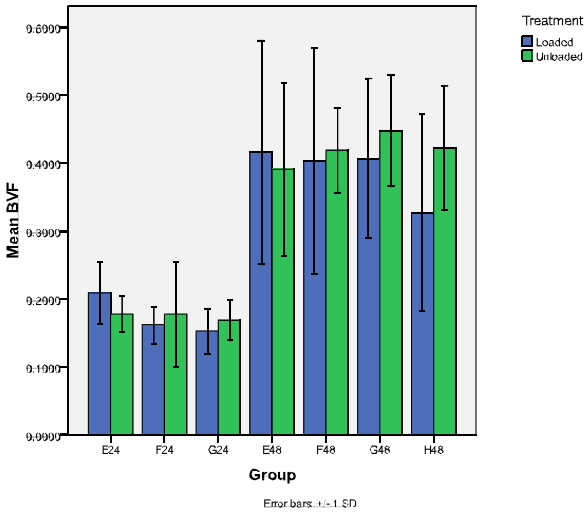

Univariate ANOVA shows the obvious significant differences between groups at 48 days of healing and those at 24 days, but nothing significant between the different load initiation groups.

Tissue Mineral Density (TMD)

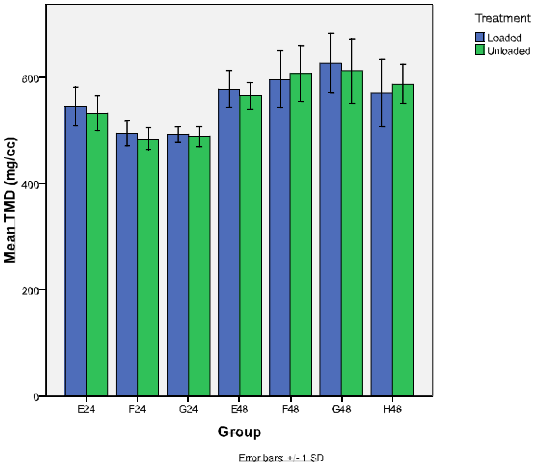

Univariate ANOVA shows nothing significant between load and control within any given group, nor across groups.

Biomechanical Testing

Specimens were tested to failure in tension using an MTS servo-hydraulic materials testing system. To ensure that the fracture gap was undisturbed throughout preparation for the tensile test, a secondary, metal fixator was placed on the two inner pins, stabilizing the fracture gap during the potting procedure. Once the specimens were successfully potted, they were then tested to failure in uniaxial tension. A prepared specimen illustrated below, as well as one that has the temporary fixator removed and is placed in the materials testing system.

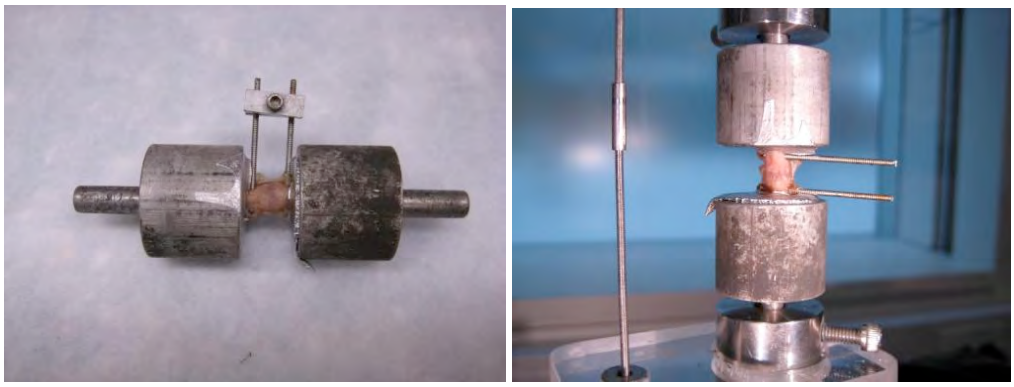

A custom MATLAB (Mathworks, Natick, MA) script was then used to determine the stiffness, ultimate tensile load, failure displacement, and energy to failure from the load/deformation curves generated during the tests. Data from measures of ultimate load to failure are shown below.

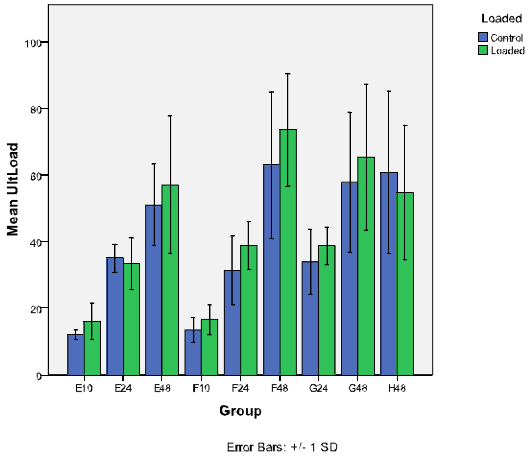

A univariate ANOVA with Group and Load as fixed factors was then run. Group signifies the subgroup of load protocol (E,F,G,H) as well as healing time (10,24,48 days post-op). For instance a "Group" is all data from E10. Therefore the ANOVA compared the mean ultimate loads within the group (E10, F10, E24, F24, G24, E48, F48, G48, H48) as well as control vs loaded.

Group was found to be significant and that lead us to perform pairwise comparisons (using Bonferroni Correction) of the groups in general (without breaking the data up into loaded and control). There was no significant difference between treatment groups at a given healing timepoint. For instance, looking at all the data within the animals sacrificed 48 days post-op, load did not have a significant effect.

The same trend of results were found for stiffness. Of course, when collapsed across load/no-load, there was a significant effect of time. The later times (48 days) were stiffer than the earlier calluses, as would be expected.

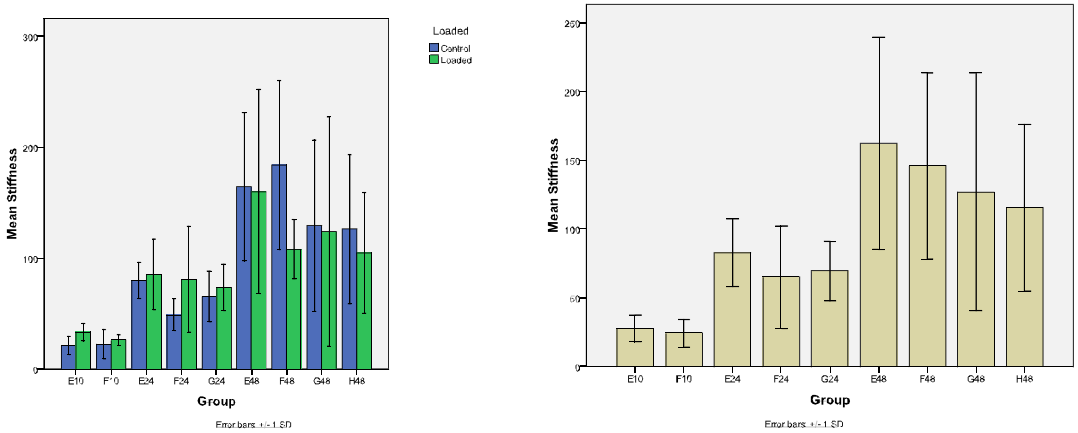

Taken together, these results and others from the mechanical testing demonstrated that the introduction of cells into the local fracture site, retarded the repair process although in time, they regenerate tissue became more mineralized and mature. All of the histologic results confirmed these observation.

Key Research Findings and Conclusions/Interpretations

1. The timing of the application of a mechanical stimulus can play a role in the progression of healing in a fractured bone.
    a. An axially applied displacement had a beneficial effect on mineralization and the progression of remodeling in animals that were stimulated after ten days
    b. Loading on day three after fracture was shown to be deleterious to the repair process
2. Mesenchymal stem cells, injected systemically into these animals, took residence in the marrow spaces of all the animals after 48 days, with the exception of the animals stimulated starting on day ten.
    a. The data suggest that exogenous cells (when given at certain times) may not be beneficial for fracture healing, as they may compete with endogenous cells or regulatory processes
3. PCR array demonstrated that in tissues in which an applied stimulus was introduced, substantial changes in the expression of several important factors, both locally and systemically occurred. These factors may represent targets for the promotion of healing or for the homing of progenitor cells.
4. Based on the findings of Phase I studies and analysis, it is clear that mechanical loading and the introduction of systemic progenitor cells can have a substantial effect on fracture repair. However, the timing is critical and needs to be considered when developing novel treatment strategies
5. Surprisingly, locally delivered progenitor cells in a demineralized matrix can have a deleterious effect on fracture repair.

6. The addition of mechanical stimulation to a fracture repair site in which progenitor cells were locally delivered, had no effect on the repair process.
7. Given the apparent deleterious influence of locally delivered progenitor cells, it is likely critical to examine several factors that may be associated with repair enhancement:
    a. The number of cells delivered may influence the repair process. Delivering a large number of cells may interfere with normal endogenous processes.
    b. The available nutrients or neovascular regeneration in the region of cell delivery may be a critical factor. Essentially, the delivery of a large number of cells, without the necessary vascular support may result in massive cell death and subsequent deleterious effects.
    c. If an optimal number of cells could be delivered and supported by timely, new vascularity, they may actually promote enhanced healing. This concept, however, must be tested in future studies.

Reportable Outcomes

Papers and Abstracts

Aaron S. Weaver. The Effect of Mechanical Stimulation on Bone Fracture Healing: Changes in Callus Morphology and Mesenchymal Stem Cell Homing. Doctoral Dissertation. University of Michigan September 2008.

Weaver, Aaron S.; Alford, Andrea I.; Hankenson, Kurt D.; Su, Yu-Ping; Begun, Dana L.; Kreider, Jaclynn M.; Ablowitz, Stephanie A.; Kilbourn, Michael R.; Goldstein, Steven A. "Influence of controlled mechanical stimulation and donor mesenchymal progenitor cells on fracture healing." Transactions of the ORS 54th Annual Meeting, San Francisco, CA., volume 33, paper # 396, 2008.

Weaver AS, Su YP, Begun DL, Miller JD, Alford AI, Goldstein SA. "The Effects of Axial Displacement on Fracture Callus Morphology and MSC Homing on the Timing of Application." Submitted to Bone (in revision).

Additional funding related to topic and area of investigation acquired as a result of the work.

National Institutes of Health (R01AR51504), "Mechanical Factors and Cellular Responsiveness in Fracture Repair," (S. Goldstein, Principal Investigator), $1,125,000 TDC, 1/1/07-11/30/11

Students trained

Aaron Weaver PhD (graduate research assistant, doctoral studies supported by the program)
Aaron Swick MS. (graduate research assistant)
Dana Begun BS (PhD student who participated in project)
Yu-Ping Su MD (postdoctoral fellow who participated in project)

Conclusions

As summarized in the body of the report, our studies revealed that the application of mechanical load can influence the character and rate of fracture repair. This influence, however, is dependent on timing of load application. In fact, loads applied at day three were shown to be detrimental to the repair process. This is likely due to the disruptive effect on early neovasularization and granulation tissue formation. In contrast, loads applied after 10 days had a positive effect. Furthermore, the introduction of systemic progenitor cells resulted in mixed results. While the cells found their way, preferentially, to the repair site when stimulated, their influence was not always positive. We hypothesize that this was due to a competition with endogenous cells or factors. Furthermore, immunohistochemistry demonstrated that the cells most often located to the marrow and likely contributed through the production of soluble factors and not by differentiating to matrix producing cells. Taken together, these results suggest that the use of mechanical stimulation and potentially systemically introduced cells, the fate of fracture repair can be substantially altered. Importantly, the local delivery of a large number of progenitor cells had a deleterious effect on repair. The addition of load had no further influence. This suggests that they may have interfered with endogenous processes, or more likely, were not sufficiently supported by neovascularity, leading to their death and associated negative impact on the repair process. These results in aggregate demonstrate a variety of important parameters that may lead to new or revised strategies for enhancing fracture repair. It is likely that mechanical load and delivered cells can substantially augment repair when delivered at the right time and with an appropriately increased vascular supply to support the cells. Future studies should focus on these issues. Importantly, these studies also demonstrate useful models for the study of fracture repair and its stimulation.

References

1. Birnbaum T, Roider J, Schankin CJ, Padovan CS, Schichor C, Goldbrunner R, Straube A. Malignant gliomas actively recruit bone marrow stromal cells by secreting angiogenic cytokines. Journal of Neuro-Oncology 2007;83: 241-247.
2. Croitoru-Lamoury J, Lamoury FMJ, Zaunders JJ, Veas LA, Brew BJ. Human mesenchymal stem cells constitutively express chemokines and chemokine receptors that can be upregulated by cytokines, IFN-beta, and Copaxone. Journal of Interferon and Cytokine Research 2007;27: 53-64.
3. Dimitriou R, Tsiridis E, Giannoudis PV. Current concepts of molecular aspects of bone healing. Injury-International Journal of the Care of the Injured 2005;36: 1392-1404.

4. Fiedler J, Brill C, Blum WF, Brenner RE. IGF-I and IGF-II stimulate directed cell migration of bone-marrow-derived human mesenchymal progenitor cells. Biochemical and Biophysical Research Communications 2006;345: 1177-1183.
5. Fiedler J, Etzel N, Brenner RE. To go or not to go: Migration of human mesenchymal progenitor cells stimulated by isoforms of PDGF. Journal of Cellular Biochemistry 2004;93: 990-998.
6. Fiedler J, Leucht F, Waltenberger J, Dehio C, Brenner RE. VEGF-A and PlGF-1 stimulate chemotactic migration of human mesenchymal progenitor cells. Biochemical and Biophysical Research Communications 2005;334: 561-568.
7. Fiedler J, Roderer G, Gunther KP, Brenner RE. BMP-2, BMP-4, and PDGF-bb stimulate chemotactic migration of primary human mesenchymal progenitor cells. Journal of Cellular Biochemistry 2002;87: 305-312.
8. Ji JF, He BP, Dheen ST, Tay SSW. Interactions of chemokines and chemokine receptors mediate the migration of mesenchymal stem cells to the impaired site in the brain after hypoglossal nerve injury. Stem Cells 2004;22: 415-427.
9. Jung Y, Wang J, Schneider A, Sun YX, Koh-Paige AJ, Osman NI, McCauley LK, Taichman RS. Regulation of SDF-1 (CXCL12) production by osteoblasts; a possible mechanism for stem cell homing. Bone 2006;38: 497-508.
10. Karadag A, Fisher LW. Bone sialoprotein enhances migration of bone marrow stromal cells through matrices by bridging MMP-2 to alpha(v)beta3-integrin. J Bone Miner Res 2006;21: 1627-36.
11. Kucia M, Wojakowski W, Reca R, Machalinski B, Gozdzik J, Majka M, Baran J, Ratajczak J, Ratajczak MZ. The migration of bone marrow-derived non-hematopoietic tissue-committed stem cells is regulated in an SDF-1-, HGF-, and LIF-dependent manner. Archivum Immunologiae Et Therapiae Experimentalis 2006;54: 121-135.
12. Li Y, Yu X, Lin S, Li X, Zhang S, Song YH. Insulin-like growth factor 1 enhances the migratory capacity of mesenchymal stem cells. Biochem Biophys Res Commun 2007;356: 780-4.
13. Lind M, Eriksen EF, Bunger C. Bone morphogenetic protein-2 but not bone morphogenetic protein-4 and -6 stimulates chemotactic migration of human osteoblasts, human marrow osteoblasts, and U2-OS cells. Bone 1996;18: 53-57.
14. Metheny-Barlow LJ, Tian S, Hayes AJ, Li LY. Direct chemotactic action of angiopoietin-1 on mesenchymal cells in the presence of VEGF. Microvasc Res 2004;68: 221-30.
15. Motoo Y, Xie MJ, Mouri H, Sawabu N. Expression of interleukin-8 in human obstructive pancreatitis. Jop. Journal of the Pancreas 2004;5: 138-144.
16. Ozaki Y, Nishimura M, Sekiya K, Suehiro F, Kanawa M, Nikawa H, Hamada T, Kato Y. Comprehensive analysis of chemotactic factors for bone marrow mesenchymal stem cells. Stem Cells and Development 2007;16: 119-129.
17. Ponte AL, Marais E, Gallay N, Langonne A, Delorme B, Herault O, Charbord P, Domenech J. The in vitro migration capacity of human bone marrow mesenchymal stem cells: Comparison of chemokine and growth factor chemotactic activities. Stem Cells 2007;25: 1737-1745.
18. Ringe J, Strassburg S, Neumann K, Endres M, Notter M, Burmester GR, Kaps C, Sittinger M. Towards in situ tissue repair: Human mesenchymal stem cells express chemokine receptors CXCR1, CXCR2 and CCR2. and migrate upon stimulation with

CXCL8 but not CCL2. Journal of Cellular Biochemistry 2007;101: 135-146.
19. Schantz JT, Chim H, Whiteman M. Cell Guidance in Tissue Engineering: SDF-1 Mediates Site-Directed Homing of Mesenchymal Stem Cells within Three-Dimensional Polycaprolactone Scaffolds. Tissue Eng 2007;13: 2615-24.
20. Schmidt A, Ladage D, Schinkothe T, Klausmann U, Ulrichsa C, Klinz FJ, Brixius K, Arnhold S, Desai B, Mehlhorn U, Schwinger RHG, Staib P, Addicks K, Bloch W. Basic fibroblast growth factor controls migration in human mesenchymal stem cells. Stem Cells 2006;24: 1750-1758.
21. Sordi V, Malosio ML, Marchesi F, Mercalli A, Melzi R, Giordano T, Belmonte N, Ferrari G, Leone BE, Bertuzzi F, Zerbini G, Allavena P, Bonifacio E, Piemonti L. Bone marrow mesenchymal stem cells express a restricted set of functionally active chemokine receptors capable of promoting migration to pancreatic islets. Blood 2005;106: 419-427.
22. Tamai N, Myoui A, Hirao M, Kaito T, Ochi T, Tanaka J, Takaoka K, Yoshikawa H. A new biotechnology for articular cartilage repair: subchondral implantation of a composite of interconnected porous hydroxyapatite, synthetic polymer (PLA-PEG), and bone morphogenetic protein-2 (rhBMP-2). Osteoarthritis and Cartilage 2005;13: 405-417.
23. Thibault MM, Buschmann MD. Migration of bone marrow stromal cells in 3D: 4 color methodology reveals spatially and temporally coordinated events. Cell Motil Cytoskeleton 2006;63: 725-40.
24. Thibault MM, Hoemann CD, Buschmann MD. Fibronectin, vitronectin, and collagen I induce chemotaxis and haptotaxis of human and rabbit mesenchymal stem cells in a standardized transmembrane assay. Stem Cells Dev 2007;16: 489-502.
25. Wang L, Li Y, Chen X, Chen J, Gautam SC, Xu Y, Chopp M. MCP-1, MIP-1, IL- 8 and ischemic cerebral tissue enhance human bone marrow stromal cell migration in interface culture. Hematology 2002;7: 113-117.
26. Wang L, Li Y, Gautam SC, Zhang ZG, Lu M, Chopp M. Ischemic cerebral tissue and MCP-1 enhance rat bone marrow stromal cell migration in interface culture. Experimental Hematology 2002;30: 831-836.
27. Wynn RF, Hart CA, Corradi-Perini C, O'Neill L, Evans CA, Wraith JE, Fairbairn LJ, Bellantuono I. A small proportion of mesenchymal stem cells strongly expresses functionally active CXCR4 receptor capable of promoting migration to bone marrow. Blood 2004;104: 2643-2645.
28. Claes L, Eckert-Hubner K, Augat P. The effect of mechanical stability on local vascularization and tissue differentiation in callus healing. J Orthop Res 2002;20: 1099-105.
29. Wallace AL, Draper ER, Strachan RK, McCarthy ID, Hughes SP. The vascular response to fracture micromovement. Clin Orthop Relat Res 1994: 281-90.
30. Rhinelander FW. Tibial blood supply in relation to fracture healing. Clin Orthop Relat Res 1974: 34-81.
31. Gardner MJ, van der Meulen MC, Demetrakopoulos D, Wright TM, Myers ER, Bostrom MP. In vivo cyclic axial compression affects bone healing in the mouse tibia. J Orthop Res 2006;24: 1679-86.
32. Li KW, Wang AS, Sah RL. Microenvironment regulation of extracellular signalregulated kinase activity in chondrocytes: effects of culture configuration, interleukin-1, and compressive stress. Arthritis Rheum 2003;48: 689-99.
33. Sah RL, Kim YJ, Doong JY, Grodzinsky AJ, Plaas AH, Sandy JD. Biosynthetic

response of cartilage explants to dynamic compression. J Orthop Res 1989;7: 619-36.
34. Case ND, Duty AO, Ratcliffe A, Muller R, Guldberg RE. Bone formation on tissue-engineered cartilage constructs in vivo: effects of chondrocyte viability and mechanical loading. Tissue Eng 2003;9: 587-96.
35. Kraus KH, Kirker-Head C. Mesenchymal stem cells and bone regeneration. Vet Surg 2006;35: 232-42.
36. Devine SM, Bartholomew AM, Mahmud N, Nelson M, Patil S, Hardy W,Sturgeon C, Hewett T, Chung T, Stock W, Sher D, Weissman S, Ferrer K, Mosca J,Deans R, Moseley A, Hoffman R. Mesenchymal stem cells are capable of homing to thebone marrow of non-human primates following systemic infusion. Exp Hematol 2001;29: 244-55.
37. Pereira RF, Halford KW, O'Hara MD, Leeper DB, Sokolov BP, Pollard MD,Bagasra O, Prockop DJ. Cultured adherent cells from marrow can serve as long-lasting precursor cells for bone, cartilage, and lung in irradiated mice. Proc Natl Acad Sci U S A 1995;92: 4857-61.
38. Devine SM. Mesenchymal stem cells: will they have a role in the clinic? J Cell Biochem Suppl 2002;38: 73-9.

Influence of controlled mechanical stimulation and donor mesenchymal progenitor cells on fracture healing

Aaron S. Weaver[1], Andrea I. Alford[1], Kurt D. Hankenson[3], Yu-Ping Su[1], Dana L. Begun[1], Jaclynn M. Kreider[1], Stephanie A. Ablowitz[1], Michael R. Kilbourn[2], Steven A. Goldstein[1]

[1]Orthopaedic Surgery, University of Michigan, Ann Arbor, MI; [2]Radiology, University of Michigan, Ann Arbor, MI; [3]Animal Biology, University of Pennsylvania, Philadelphia, PA

asweaver@umich.edu

Introduction: Fracture healing is a complex process involving numerous cell types, and a variety of spatially and temporally related regulators. Mechanical forces have been shown to play an important role in the extent and character of the repair process. While prior studies have investigated the effect of physical forces on cell differentiation, biofactor expression, and mechanical competence of repair, the mechanosensory and response mechanisms are poorly understood. The purpose of this study was to evaluate the temporal effect of a controlled mechanical environment on fracture repair. Specifically, this study was designed to investigate the timing of mechanical load and its influence on systemic mesenchymal stem cell (MSC) homing and local cell behavior during fracture repair.

Materials and Methods: Sixty-two, 6-month-old, male, Sprague-Dawley rats underwent a 2mm segmental osteotomy in the mid-diaphysis of each femur. Briefly, after a 1cm exposure and elevation of the soft tissues, four 0.062-inch diameter threaded pins were placed through predrilled holes in the diaphysis using a specialized guide. A two-piece external fixator with locking plate was then affixed to the pins, an osteotomy created with an oscillating saw, and the surrounding tissues closed.

Marrow was flushed from femora and tibiae of 2- to 4-month-old, male, green fluorescent protein (GFP) transgenic rats and cultured in standard growth medium. After 12-14 days, adherent cells were replated at a density of $0.7x10^6$ cells per 10cm culture dish, and this process was repeated to create second passage (P2) MSC. After 24 hours, the medium was removed and replaced with a serum free defined medium consisting of a 60/40 mixture of DMEM/MCDB1 (Gibco/Sigma) containing 1% antibioitic/antimycotic (Gibco), 1% LA-BSA (Sigma), 0.01% PDGF-β (Cell Signaling), .001% bFGF (Cell Signaling), and 0.05% insulin (Sigma). Systemic injections of $1x10^6$ cells in 1ml PBS were performed via the tail vein on the first loading day.

Mechanical stimulation was performed by a system that provides controlled axial displacement. The rats were placed in a sling, the fixator aligned and secured in the loading device, and the locking plate removed. Mechanical stimulation occurred for five consecutive days beginning at 0, 3, 10, or 24 days post-operative (groups A through D respectively) at a magnitude of ±8% strain and a rate of .313 Hz for 510 loading cycles. Rats were euthanized 10, 24, or 48 days post-op.

Following sacrifice, both femora were excised and scanned on a μCT (GE Health Systems) at 18μm voxels. After scanning, specimens were embedded in PMMA, cut into 5μm thick sections, mounted, and then either left unstained to look for GFP activity or stained using toluidine blue or safranin-O and fast green.

Eight additional animals were analyzed for progenitor cell migration using planar gamma imaging. ^{111}Indium was added to the cell suspension prior to injection and allowed to diffuse into the cells for 30 minutes. The suspension was then centrifuged and any free-floating ^{111}indium was removed from the supernatant. Cells were injected prior to loading as above. The animals were loaded and scanned for three consecutive days.

Ratios between loaded and unloaded limbs analyzed by μCT were calculated for all outcome variables and a student's t-test was used to determine differences in the means within groups. All experimental procedures were approved by the Committee on Use and Care of Animals.

Results: Data from the early time points indicate no change or even a slight decrease in callus formation due to load. As healing progresses, the loaded limbs show an increased callus size as can be seen from the data at day 48 (Fig. 1). In the groups loaded 0 or 3 days post-op (groups A and B), the BMD ratio remained unchanged throughout the healing process, but for the groups loaded 10 and 24 days post-surgery (groups C and D), there was an increase in BMD by day 48. The tissue mineral density across all groups and time points remained the same (data not shown) indicating that load did not influence the timing of mineralization.

Gamma images from animals injected and loaded 0 or 3 days post-op showed little sign of radioactivity at either fracture site with most of the signal concentrated in the lungs. Animals that were loaded 10 or 24 days post-op showed migration of the MSCs out of the lungs and into the fracture sites, with the appearance of preferential homing to the loaded fracture site (Fig. 2).

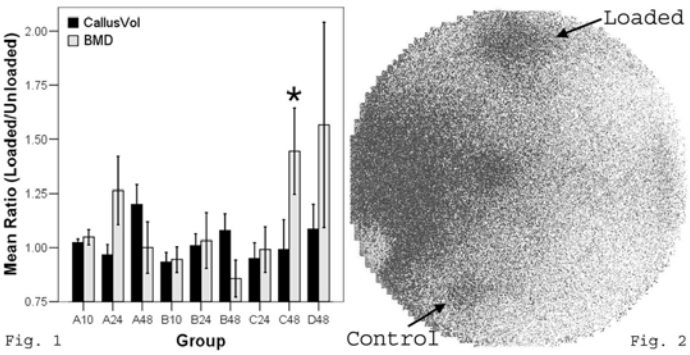

Figure 1: The callus volume ratio between the loaded and unloaded limb shows little change due to load initially, but at later time points load seems to increase callus size. BMD is unchanged in groups A and B and increases in groups C and D indicating that loading during the later stages of fracture healing may promote a higher proportion of mineral. (* = p<.05)
Figure 2: This gamma image from a rat injected and loaded 24 days post-op shows a preferential homing of the radiolabeled MSC to the loaded fracture site. There was no MSC activity found in the limbs of animals loaded 0 and 3 days post-op, while there was measurable activity in the limbs of 10 and 24-day animals.

Discussion: Load initially has little effect on callus formation, but as healing progresses, callus size is increased. The BMD data seem to indicate that when loading is initiated early, load does not change the proportion or degree of mineralization in the callus. If loading is delayed however, a higher proportion of mineral may form in the callus by day 48, as indicated by results from groups loaded 10 and 24 days post-op. Due to current sample size limitations, only the BMD value for the C48 group reached statistical significance.

The gamma images show that we are able to measure MSC migration to the fracture sites, and early data suggest that migration is affected by the local mechanical environment. The scans from time points early in the fracture healing process showed little migration to the osteotomies indicating a lack of expression of factors influencing MSC migration. Confirmation of the homing dynamics and the contribution of the migrating cells to the repair process will be derived from histologic analysis of GFP fluorescence.

Acknowledgements: We thank Kathy Sweet, Charles Roehm, Dennis Kayner, Rochelle Taylor, John Baker, Michael Paschke, Phillip Sherman, Carole Quesada, Ralph Zade, and Eric Lee for their contributions to this project. DOD (AIBS-003530)

Elsevier Editorial System(tm) for Bone
Manuscript Draft

Manuscript Number:

Title: The Effects of Axial Displacement on Fracture Callus Morphology and MSC Homing Depend on the Timing of Application

Article Type: Original Full Length Article

Keywords: mesenchymal stem cells; mechanical strain; fracture healing

Corresponding Author: Dr. Aaron S Weaver, Ph.D.

Corresponding Author's Institution: National Aeronautics and Space Administration

First Author: Aaron S Weaver, Ph.D.

Order of Authors: Aaron S Weaver, Ph.D.; Yu-Ping Su, M.D.; Dana L Begun; Joshua D Miller, M.D., Ph.D.; Andrea I Alford, Ph.D.; Steven A Goldstein, Ph.D.

Abstract: The local mechanical environment and the availability of mesenchymal stem cells (MSCs) have both been shown to be important factors in bone fracture healing. This study was designed to investigate how the timing of an applied axial displacement across a healing fracture affects callus properties as well as the migration of systemically introduced MSCs. Bilateral osteotomies were created in male, Sprague-Dawley rats. Exogenous MSCs were injected via the tail vein, and a controlled micro-motion was applied to one defect starting 0, 3, 10, or 24 days after surgery. The results showed that fractures stimulated 10 days after surgery had more mineral, less cartilage, and greater mechanical properties at 48 days than other groups. Populations of MSCs were found in osteotomies 48 days after surgery, with the exception of the group that was stimulated 10 days after surgery. These results demonstrate that the timing of mechanical stimulation affects the physical properties of the callus and the migration of MSCs to the fracture site.

Suggested Reviewers: Cato Laurencin M.D., Ph.D.

James Dennis Ph.D.

Opposed Reviewers:

Cover Letter

Aaron Weaver
21000 Brookpark Rd. MS 110-3
Cleveland, OH 44135
Email: Aaron.S.Weaver@nasa.gov
July 9, 2009

Dear Dr. Einhorn,

Attached is our journal article entitled "The Effects of Axial Displacement on Fracture Callus Morphology and MSC Homing Depend on the Timing of Application." We are submitting this article for consideration of publication in *Bone*.

This work represents a continuation of the studies at the University of Michigan focused on the influence of mechanical factors on fracture repair and the interplay between local mechanical conditions and progenitor cell behavior. We believe the work will be of interest to the Orthopaedic community and appreciate the opportunity for the paper to be considered for publication.

Sincerely,

Aaron Weaver
Biomedical Engineer
NASA Glenn Research Center

The Effects of Axial Displacement on Fracture Callus Morphology and MSC Homing Depend on the Timing of Application

Aaron S. Weaver[1,2], Yu-Ping Su[1,3], Dana L. Begun[1], Joshua D. Miller[1], Andrea I. Alford[1], Steven A. Goldstein[1]

[1]University of Michigan, Orthopaedic Research Laboratory, Ann Arbor, MI

[2]National Aeronautics and Space Administration, Glenn Research Center, Cleveland, OH

[3]National Yang-Ming University, School of Medicine, Department of Surgery, Taipei, Taiwan

Steven Goldstein

University of Michigan

Orthopaedic Research Lab

109 Zina Pitcher Pl

Room 2001

Ann Arbor, MI 48109

Abstract

The local mechanical environment and the availability of mesenchymal stem cells (MSCs) have both been shown to be important factors in bone fracture healing. This study was designed to investigate how the timing of an applied axial displacement across a healing fracture affects callus properties as well as the migration of systemically introduced MSCs. Bilateral osteotomies were created in male, Sprague-Dawley rats. Exogenous MSCs were injected via the tail vein, and a controlled micro-motion was applied to one defect starting 0, 3, 10, or 24 days after surgery. The results showed that fractures stimulated 10 days after surgery had more mineral, less cartilage, and greater mechanical properties at 48 days than other groups. Populations of MSCs were found in osteotomies 48 days after surgery, with the exception of the group that was stimulated 10 days after surgery. These results demonstrate that the timing of mechanical stimulation affects the physical properties of the callus and the migration of MSCs to the fracture site.

Keywords: mesenchymal stem cells, mechanical strain, fracture healing.

Introduction

Published data demonstrates that the local mechanical environment contributes significantly to the progress of fracture repair. Small, controlled displacements can increase bone formation [1], callus size [2, 3], and tensile strength [2]. Moreover, fractures subjected to cyclic compression demonstrate higher torque and energy to failure, higher torsional stiffness, more advanced tissue differentiation, and more complete bony bridging than when rigidly fixed [4, 5].

The availability of mesenchymal stem cells (MSCs) at the fracture site is also an important factor in healing. It may be advantageous to use MSCs to augment fracture repair, since they are involved in every aspect of bone regeneration [6]. Exogenous MSCs have been used to repair critical sized, segmental bone defects in animal models [6-9], and they have been shown to increase bone mineral content and growth velocity in children with severe osteogenesis imperfecta [10, 11]. MSCs have also been used to treat defects in tissues other than bone including traumatic brain injury [12, 13], infarcted myocardium [14], and cerebral ischemia [15, 16], demonstrating their diverse promise for tissue repair.

Considering the influence of both progenitor cell availability and the mechanical environment on healing progression, their interplay on callus properties and cell migration to the site of repair may be critical to the quality of healing. The purpose of this study was to evaluate the temporal effect of a controlled mechanical environment on fracture repair in concert with systemic cell delivery. Specifically, this study was designed to investigate how the timing of an applied axial displacement following a femoral osteotomy affects callus morphology and the mechanical properties of the healing fracture site. We also evaluated the migration of systemically introduced, exogenous MSCs to determine if the timing of the applied displacement has an effect on the homing of these cells to the fracture site.

Methods

Animal Surgery and Mechanical Stimulation

One hundred sixteen, six-month-old, male, Sprague-Dawley rats underwent a 2mm segmental osteotomy in the mid-diaphysis of each femur (Figure 1). Briefly, after a 1cm exposure and elevation of the soft tissues, four 0.062-inch diameter threaded pins were placed through predrilled holes made in the diaphysis using a specialized guide. A two-piece external fixator with locking plate was then affixed to the pins, and an osteotomy was created with an oscillating saw under constant saline irrigation. All experimental procedures were approved by the University of Michigan Committee on Use and Care of Animals.

Axial mechanical stimulation was performed with a system that provides controlled axial motion with displacement monitored by a linear variable differential transformer (LVDT). The rats were placed in a sling so that the fixator could be properly aligned, and the locking plate was removed once it was secured in the loading device (Figure 1). Axial displacement was applied to one randomly chosen limb, while the other femur served as a contralateral control. Mechanical stimulation occurred for five consecutive days beginning at 0, 3, 10, or 24 days post-operatively (groups A through D respectively) at a magnitude of ±8% strain (±0.16 mm) and a rate of 0.313 Hz for 510 loading cycles. Rats were euthanized 10, 24, or 48 days post-operatively (Table 1).

MSC Culture and Injection

Bone marrow was harvested from 2- to 4-month-old green fluorescent protein (GFP) transgenic rats and the cells were cultured in Dulbecco's Modified Eagle Medium (DMEM, Invitrogen, Carlsbad, CA) containing 10% fetal bovine serum (Fisher Scientific, Waltham, MA) and 1% antibioitic/antimycotic (Invitrogen) at 37°C, in 5% CO_2, and 95% humidity. In order to maintain the influence of non-adherent cells, half of the total volume of culture medium was

replaced every three to four days. After 12-14 days, the cells were released from the cell culture plate using 0.25% trypsin containing 1 mM EDTA, and the cells were replated at 700,000 cells per 10cm culture dish. After reaching confluence, the cells were passaged again. Twenty-four hours later, the growth medium was removed and replaced with a serum free defined medium consisting of a 60%/40% mixture of DMEM/MCDB201 (Invitrogen/Sigma-Aldrich, St. Louis, MO) containing 1% antibioitic/antimycotic (Invitrogen), 1% linoleic acid bovine serum albumin (Sigma), 0.01% platelet-derived growth factor-β (Cell Signaling Technology, Danvers, MA), 0.001% basic fibroblast growth factor (Cell Signaling), and 0.05% insulin (Sigma) [17]. In preparation for injection, cells were trypsinized and resuspended in 1ml PBS at 1 million cells per ml per injection. Injections were performed via the tail vein immediately before the first application of axial displacement, with the exception of group DNC, which recieved no cells.

Microcomputed Tomography

Immediately after sacrifice, both femora were excised and the surrounding soft tissue was removed without disturbing the callus around the fracture site. Bones were scanned via *ex-vivo* micro-CT (GE Healthcare Pre-Clinical Imaging, London, ON) at a voxel size of 18μm. A region of interest (ROI) was created encompassing the 2mm osteotomy site and any remaining cortical bone was subtracted from the region. The lateral borders of the ROI were defined by visible mineralization on the outermost boundary of the callus. A threshold of 1200 was chosen for the gray scale value to define bone voxels for all specimens. Callus volume, bone volume, bone mineral content (BMC), bone mineral density (BMD), tissue mineral content (TMC), tissue mineral density (TMD), and bone volume fraction (BVF) were recorded for each osteotomy.

Histology

After sacrifice, femurs from five animals per group were placed in 10% neutral buffered

formalin for three days. The specimens were then placed into 70% ethanol until they were processed. Specimens were embedded in poly(methyl methacrylate) and cut into 5μm thick, longitudinal sections at five different levels spaced 200-300μm apart through the thickness of the bone. Sections were mounted and then either processed for immunohisochemistry as outlined below, or stained using safranin-O to identify cartilage. Fast green was used as a nuclear counter stain. Six images per section were captured at 2.5 times magnification (Axiovert 200M, Carl Zeiss, Oberkochen, Germany) and stitched together using Photoshop (Adobe, San Jose, CA). One section per level was analyzed for a total of five sections per specimen. Each image was cropped to a height of 2mm to correspond to the size of the original osteotomy, and a boundary was drawn encompassing the callus periphery to quantify the callus area per section. Areas of cartilage and bone were quantified through color thresholding in Photoshop. Bone and cartilage areas were normalized to the callus area for each section, and the values for the five sections per specimen were averaged to arrive at a cartilage/callus area and bone/callus area for each bone.

Immunohistochemistry

Slides were deacrylized in a 1:1 mixture of xylene and chloroform for 30 minutes, rehydrated through a series of alcohol baths, and decalcified in 8% formic acid for ten minutes. Next, the sections were incubated in a proteinase K solution for 30 minutes at 37°C. The proteinase K solution was rinsed by a five minute water bath, and then the endogenous peroxidases were quenched with a 10:1 mixture of methanol and 30% H_2O_2 for 30 minutes. The sections were flushed twice with distilled water and then twice covered with PBS containing 0.1% Triton X-100 (TPBS) for five minutes each. Non-specific sites were blocked using a solution of 10% normal goat serum (Vector Laboratories, Burlingame, CA), in 0.02% TPBS containing 1.5% bovine serum albumin (BSA, Sigma). Then, sections were incubated overnight

at 4°C with a rabbit anti-rat GFP antibody (Fisher Scientific) diluted 1:1000 in 0.02% TPBS containing 1.5% BSA. The slides were then rinsed with PBS and incubated with biotinylated goat anti-rabbit immunoglobin-G (Vector Laboratories) diluted 1:500 in 0.02% TPBS containing 1.5% BSA. After washing with with PBS, the slides were incubated with Vectastain Elite ABC reagent (Vector Laboratories) for 30 minutes at room temperature. Then, they were washed with PBS, incubated with stable DAB (Invitrogen) for two minutes, rinsed gently with tap water, counterstained with fast green, and cover slipped.

Torsion Testing

The femurs from the remaining animals were tested to failure in a custom designed torsion fixture. The bone ends were secured in aluminum pots with molten bismuth that was then allow to cool. The pots were fastened on each side of the testing apparatus, and the bones were hydrated with lactated ringers solution. The locking plate of the fixator was then removed, and the bones were tested to failure at a rate of 0.5 deg/sec. A custom MATLAB (Mathworks, Natick, MA) script was used to determine the stiffness, ultimate failure torque, failure twist, and energy to failure.

Statistical Analysis

All data are expressed as means ± one standard error. A two-way, repeated measures ANOVA was run for all of the data using SAS (Cary, NC). Effects of treatment (mechanically stimulated versus control) and timing of displacement initiation, as well as the interaction between treatment and timing were analyzed. A Tukey-Kramer post-hoc adjustment was used to correct for multiple comparisons. Values were considered to be statistically different at $p \leq 0.05$.

For IHC analysis, three of the five levels per bone were used for a qualitative analysis. The levels chosen (levels one, three, and five) represent a symmetric view of the whole callus. Cells

were viewed in the marrow within the medullary canal and peripheral callus and were scored. A score of zero corresponds to no cells present, a score of one represents 1-10 cells, and a score of two signifies that 11 or more cells were present in the marrow.

Results

Micro-CT analysis of callus mineralization suggests that the timing of mechanical stimulation had a significant impact on repair. Twenty-four days after surgery, fracture gaps that were stimulated on day three have less mineralized tissue than those stimulated on either day zero or day ten (Figure 2), and this difference reached significance between groups B (stimulation day 3) and C (stimulation day 10). Forty-eight days after surgery, there was more mineral in the defects displaced ten days post surgery (group C48) compared to those from the group displaced three days post surgery (group B48) (Figure 3). There is also a trend toward a higher TMD in group C48 than in B48 (data not shown). In fractures stimulated ten days after surgery, increased mineral content is associated with a significant decrease in cartilage (Figure 4). Similarly, the loaded limbs in group C48 have significantly less cartilage than their contralateral controls ($p=0.045$), while the loaded limbs in group A48 have more cartilage than their contralateral controls ($p=0.037$). There is also a difference in cartilage area between limbs stimulated at day ten and limbs that were stimulated at day zero ($p=0.031$) or day three ($p=0.015$) (Figure 5).

Figure 6 shows that stimulation starting at day three (group B10) induced more cartilage formation by day ten than did stimulation immediately after surgery (group A10). It also shows that the control limbs in the B10 group have a larger cartilage area than the controls from group A10 suggesting that locally applied loads might exert systemic effects. In animals euthanized on day 48, there is a significantly larger percentage of bone in the fracture gaps as measured by

histology on both the loaded and control sides for the animals stimulated starting on day ten (group C48) than for any other group (Figure 7). There is also more bone in the control defect of group C48 than for D48. The torsion data shows that bones from animals displaced on day ten are more stiff and stronger in torsion than bones from any other groups (Figure 8). The controls from that group are also significantly stiffer and have a higher failure torque than the control bones from animals stimulated on day 24.

IHC shows that even though there is a small number of exogenous MSCs present throughout the healing process, the largest population of cells does not appear until 48 days after surgery. At that time, MSCs are detected in large populations throughout the marrow in the medullary canal and the marrow spaces within the periosteal callus (Figure 9). This is true for all of the groups euthanized on day 48 except for the group stimulated ten days post-op (group C). It also appears that stimulation increases the number of cells in the fractured limb, as the scores for the stimulated limbs were higher than the control limbs at most time points (Table 2).

To look at the effect that the cells may have on healing, a group in which exogenous cells were not injected was compared via micro-CT and mechanical testing in torsion to the group D48. The group without cells had a higher bone volume, BMC, BMD, TMC, and BVF than the group with injected cells. Stiffness and torque to failure were also higher in the group without exogenous cells as compared to the group that had cells delivered via the tail vein (Figure 10).

Discussion

The application of an axial displacement has a definitive effect on fracture healing. Specifically, the timing of the stimulus is an important factor in determining the progression of callus morphology and mechanical properties. Differences in healing due to displacement can be seen as early as ten days after fracture. By day 24, the group that was displaced three days after

surgery (group B24) had a decrease in mineralization on the displaced side in comparison to the other groups. Forty-eight days after surgery, the group stimulated ten days post-op (group C48) had an elevated mineral content and almost no cartilage remaining on the stimulated side, while all the other groups still displayed a significant amount of cartilage.

The observation that the application of displacement soon after surgery decreased mineralization and mechanical properties compared to the animals that had displacement starting on day ten suggests that axial mechanical stimulation may not be beneficial during the initial response to fracture. Vascular supply is an important factor in determining the success of healing, and it may be necessary to allow neovascularization to progress at the site of repair before mechanical load is applied [18, 19]. Early motion at the fracture site causes the capillaries needed to support osseous tissues to constantly rupture, which promotes fibrocartilage formation since it requires less vascularization [20]. Therefore, it may be beneficial to the overall healing outcome to delay initiation of loading until new vessels have had a chance to form [21].

Our results suggest that it may be beneficial to start fracture stimulation after the inflammatory stage, when some soft tissue has had a chance to form. After the initial inflammatory response, cells that may be responsive to load, such as chondrocytes, have an opportunity to populate the fracture site. A potential beneficial response to chondrocyte loading in fracture healing has been shown previously. Scaffolds seeded with chondrocytes that were implanted in the femora of rabbits and then compressively loaded had a higher bone volume fraction than the unloaded controls [22], showing that the application of a stimulus to a chondrocyte population may encourage bone formation at the site of repair.

Our results also suggest that a local mechanical stimulus can influence callus properties in the contralateral fracture site, and that the timing of load influences the magnitude of these

systemic effects. At day ten, the animals loaded three days post-operatively (group B10) exhibited significantly more cartilage as a whole (loaded and control combined) than those loaded immediately after surgery. At day 48, the group loaded ten days post-op (group C48) had a significantly higher bone to callus ratio, stiffness, and failure torque as a whole when compared to all other groups suggesting that, in this group, the applied stimulus increased bone formation and mechanical properties in both the loaded and control defects. This is consistent with findings that skeletal injury elicits an osteogenic response at distant sites [23]. Einhorn and colleagues demonstrated markedly increased mineral apposition rates in both tibiae following surgically-induced injury to the right femur [24]. Transverse loading of the knee has also been shown to accelerate healing in defects in the tibial diaphysis [25].

The presence of GFP positive cells confirmed that donor MSC are able to migrate to the femora, where, in most cases, they establish a population in the marrow by day 48. This is consistent with other studies that have found exogenous MSCs in the bone marrow for long periods after a systemic injection [26], and they do not appear in large numbers in the first few weeks after delivery [27]. Our results also suggest that the presence of cells has a deleterious effect on the fracture healing process. The animals that had stimulation and cell delivery at day 24 exhibited less mineralization and lower mechanical properties in torsion than animals from the same group in which cells were not injected. Taken together, our histology and micro-CT results indicate a trend for a deleterious effect of exogenous MSC in all groups except the one stimulated starting on day 10 (Group C48). This group had the lowest number of exogenous MSCs present around the fracture site and also had the highest mineral content, as well as evidence of accelerated fracture healing.

A controlled, axial stimulation has a definitive effect on fracture healing, and the timing of

the application of the displacement differentially effects callus morphology and mechanical properties. Stimulation early in the repair process was not beneficial to fracture healing, but when the displacement was applied starting ten days after injury it increased mineralization, accelerated callus remodeling, and increased torsional mechanical properties in comparison to other groups. This effect was seen on both the experimental and the contralateral control defects, indicating that there may be a systemic effect from the applied stimulus. Exogenous MSCs form large populations in the marrow by 48 days after surgery. Mechanical stimulation immediately after the inflammatory phase (stimulation on day 10) seemed to prevent these cells from engrafting and also improved healing in comparison to the other groups. In addition, cell injections had a deleterious effect on fracture healing in animals that had cells delivered on day 24 (group D). These findings help to clarify the role of the timing of mechanical manipulation of fractures, and may help define parameters to be used in future fracture treatment.

Acknowledgments

We would like to thank Kathy Sweet, Bonnie Nolan, Charles Roehm, Dennis Kayner, Jaclynn Kreider, John Baker, Rochele Taylor, Michael Paschke, Stephanie Alblowitz, Ralph Zade, David Lee, Srikanth Volvalou, and Eric Lee for their enormous contributions to this work. The study was funded by grants from the Department of Defense and the National Institutes of Health (AR51504).

References

[1] Yamaji T, Ando K, Wolf S, Augat P, Claes L. The effect of micromovement on callus formation. Journal of Orthopaedic Science 2001;6:571-5.

[2] Claes LE, Wilke HJ, Augat P, Rubenacker S, Margevicius KJ. Effect of dynamization on gap healing of diaphyseal fractures under external fixation. Clinical Biomechanics 1995;10:227-34.

[3] Claes LE, Heigele CA, Neidlinger-Wilke C, Kaspar D, Seidl W, Margevicius KJ, Augat P. Effects of mechanical factors on the fracture healing process. Clin Orthop Relat R Clin Orthop Relat R 1998:S132-S147.

[4] Goodship AE, Kenwright J. The influence of induced micromovement upon the healing of experimental tibial fractures. Journal of Bone and Joint Surgery-British Volume 1985;67:650-5.

[5] Wolf JW, White AA, Panjabi MM, Southwick WO. Comparison of cyclic loading versus constant compression in the treatment of long-bone fractures in rabbits. Journal of Bone and Joint Surgery-American Volume 1981;63:805-10.

[6] Kraus KH, Kirker-Head C. Mesenchymal stem cells and bone regeneration. Vet Surg 2006;35:232-42.

[7] Arinzeh TL, Peter SJ, Archambault MP, van den Bos C, Gordon S, Kraus K, Smith A, Kadiyala S. Allogeneic mesenchymal stem cells regenerate bone in a critical-sized canine segmental defect. J Bone Joint Surg Am 2003;85-A:1927-35.

[8] Kon E, Muraglia A, Corsi A, Bianco P, Marcacci M, Martin I, Boyde A, Ruspantini I, Chistolini P, Rocca M, Giardino R, Cancedda R, Quarto R. Autologous bone marrow

stromal cells loaded onto porous hydroxyapatite ceramic accelerate bone repair in critical-size defects of sheep long bones. J Biomed Mater Res 2000;49:328-37.

[9] Petite H, Viateau V, Bensaid W, Meunier A, de Pollak C, Bourguignon M, Oudina K, Sedel L, Guillemin G. Tissue-engineered bone regeneration. Nat Biotechnol 2000;18:959-63.

[10] Horwitz EM, Prockop DJ, Fitzpatrick LA, Koo WW, Gordon PL, Neel M, Sussman M, Orchard P, Marx JC, Pyeritz RE, Brenner MK. Transplantability and therapeutic effects of bone marrow-derived mesenchymal cells in children with osteogenesis imperfecta. Nat Med 1999;5:309-13.

[11] Horwitz EM, Gordon PL, Koo WK, Marx JC, Neel MD, McNall RY, Muul L, Hofmann T. Isolated allogeneic bone marrow-derived mesenchymal cells engraft and stimulate growth in children with osteogenesis imperfecta: Implications for cell therapy of bone. Proc Natl Acad Sci U S A 2002;99:8932-7.

[12] Lu D, Mahmood A, Wang L, Li Y, Lu M, Chopp M. Adult bone marrow stromal cells administered intravenously to rats after traumatic brain injury migrate into brain and improve neurological outcome. Neuroreport 2001;12:559-63.

[13] Mahmood A, Lu D, Wang L, Li Y, Lu M, Chopp M. Treatment of traumatic brain injury in female rats with intravenous administration of bone marrow stromal cells. Neurosurgery 2001;49:1196-203.

[14] Orlic D, Kajstura J, Chimenti S, Jakoniuk I, Anderson SM, Li B, Pickel J, McKay R, Nadal-Ginard B, Bodine DM, Leri A, Anversa P. Bone marrow cells regenerate infarcted myocardium. Nature 2001;410:701-5.

[15] Chen J, Li Y, Wang L, Lu M, Zhang X, Chopp M. Therapeutic benefit of intracerebral transplantation of bone marrow stromal cells after cerebral ischemia in rats. J Neurol Sci 2001;189:49-57.

[16] Wang L, Li Y, Gautam SC, Zhang ZG, Lu M, Chopp M. Ischemic cerebral tissue and MCP-1 enhance rat bone marrow stromal cell migration in interface culture. Experimental Hematology 2002;30:831-6.

[17] Lennon DP, Haynesworth SE, Young RG, Dennis JE, Caplan AI. A Chemically-Defined Medium Supports in-Vitro Proliferation and Maintains the Osteochondral Potential of Rat Marrow-Derived Mesenchymal Stem-Cells. Exp Cell Res Exp Cell Res 1995;219:211-22.

[18] Claes L, Eckert-Hubner K, Augat P. The effect of mechanical stability on local vascularization and tissue differentiation in callus healing. J Orthop Res 2002;20:1099-105.

[19] Wallace AL, Draper ER, Strachan RK, McCarthy ID, Hughes SP. The vascular response to fracture micromovement. Clin Orthop Relat Res 1994:281-90.

[20] Rhinelander FW. Tibial blood supply in relation to fracture healing. Clin Orthop Relat Res 1974:34-81.

[21] Gardner MJ, van der Meulen MC, Demetrakopoulos D, Wright TM, Myers ER, Bostrom MP. In vivo cyclic axial compression affects bone healing in the mouse tibia. J Orthop Res 2006;24:1679-86.

[22] Case ND, Duty AO, Ratcliffe A, Muller R, Guldberg RE. Bone formation on tissue-engineered cartilage constructs in vivo: effects of chondrocyte viability and mechanical loading. Tissue Eng 2003;9:587-96.

[23] Lucas TS, Bab IA, Lian JB, Stein GS, Jazrawi L, Majeska RJ, ttar-Namdar M, Einhorn TA. Stimulation of systemic bone formation induced by experimental blood loss. Clin Orthop Relat Res 1997:267-75.

[24] Einhorn TA, Simon G, Devlin VJ, Warman J, Sidhu SP, Vigorita VJ. The osteogenic response to distant skeletal injury. J Bone Joint Surg Am 1990;72:1374-8.

[25] Zhang P, Sun Q, Turner CH, Yokota H. Knee loading accelerates bone healing in mice. J Bone Miner Res 2007;22:1979-87.

[26] Devine SM, Bartholomew AM, Mahmud N, Nelson M, Patil S, Hardy W, Sturgeon C, Hewett T, Chung T, Stock W, Sher D, Weissman S, Ferrer K, Mosca J, Deans R, Moseley A, Hoffman R. Mesenchymal stem cells are capable of homing to the bone marrow of non-human primates following systemic infusion. Exp Hematol 2001;29:244-55.

[27] Pereira RF, Halford KW, O'Hara MD, Leeper DB, Sokolov BP, Pollard MD, Bagasra O, Prockop DJ. Cultured adherent cells from marrow can serve as long-lasting precursor cells for bone, cartilage, and lung in irradiated mice. Proc Natl Acad Sci U S A 1995;92:4857-61.

Table and Figure Descriptions

Table 1: Nomenclature and Expermiental Group Sizes - This table shows the nomenclature for each group used in the study. The letters correspond to the timing of mechanical stimulation, and the numbers correspond to the day of euthanasia. The numbers in parentheses show the number of animals that were entered into the study for micro-CT, histology, and torsion testing.

Table 2: Amount of MSCs in the Marrow Spaces - The scores for the amount of MSCs in the marrow spaces of the displaced and control limbs for each group show the stimulated limbs have more cellular activity in the marrow when compared to the unstimulated control limbs. The number of cells also increases with the amount of time after injection (i.e. A48>A24>A10), except in group C, which had cell delivery and axial displacement begin ten days after surgery.

Figure 1: Overview of Surgery and Fixture for Axial Displacement - A two-millimeter segmental osteotomy was made at the mid-diaphysis of each femur (a). The fractures were stabilized using four threaded pins and a two-piece fixator that is locked in a rigid configuration for normal ambulation (b, c). During axial stimulation, the rat was anesthetized, placed in a sling, and the fixator was aligned with the fixture clamp (d). The close-up view of the fixator shows the two unlocked halves during stimulation (e).

Figure 2: BMD 24 Days After Surgery - 24 days after surgery, fractures stimulated at three days post-op (B24) have reduced BMD compared to to those displaced immediately after (A24) or ten days after surgery (C24) suggesting that mechanical stimulation during the inflammatory stage of healing leads to a subsequent reduction in callus mineralization.

Figure 3: BMD 24 Days After Surgery - BMD is significantly higher in Group C (displacement beginning ten days post-op) versus Group B (displacement beginning three days post-op) 48 days after surgery. In the later stages of healing, the mineral content is higher on the

displaced side in the animals loaded ten days post-operatively than those at other stimulation time points. This reached a significant increase over the defects displaced three days post-op, since the mineral levels in those gaps were slightly depressed compared to the other groups.

Figure 4: Histology for the Group Stimulated Ten Days After Surgery (Group C48) - When the axial displacement is started ten days after surgery, the stimulated limbs have no cartilage and have bony bridging by day 48 (shown above). The unstimulated controls have a substantial amount of bone, but still contain distinct areas of cartilage (in red). The figure shows: (a) a central section of a stimulated gap, (b) a peripheral section of a stimulated gap, (c) a central section of a control gap, and (d) a peripheral section of a control gap. Note that the difference in color between the top and the bottom images are an artifact of the staining procedure.

Figure 5: Cartilage area in animals euthanized 48 days post surgery - After 48 days, there is cartilage remaining in all groups, both stimulated and control, except for the gaps stimulated ten days after surgery (group C48). In these defects there is almost no cartilage remaining. The differences were significant between the displaced limbs of A48 and B48 in comparison to C48. There is also a significant difference between the displaced and contralateral control in group C48 ($p=0.045$, sig not shown), with the displaced side containing significantly less cartilage than the control. There is also more cartilage in the displaced side in group A48 when compared to the contralateral control ($p=0.037$, sig not shown).

Figure 6: Histology Suggests a Systemic Effect - Histology shows differences between control limbs at day ten, suggesting a systemic effect. For animals euthanized ten days after surgery, there is an overall increase in cartilage area (stimulated and control combined) in the group stimulated three days after surgery (group B10) when compared to defects from animals stimulated immediately after surgery (group A10) ($p=0.002$). The control gaps from these

animals also display an increased amount of cartilage (shown above), suggesting that there may be a systemic effect due to load.

Figure 7: Bone Formation Suggests a Systemic Effect - Histology shows differences in normalized bone area from animals euthanized on day 48. The group loaded ten days after surgery (C48) has a higher percentage of bone as a whole (stimulated and control limbs considered together) than any other group ($p=0.005$ with group A, $p=0.010$ with group B, and $p=0.009$ with group D). There is also more bone in the control gap of C48 than in the control gap of D48 ($*p=0.011$). These results suggest that the applied stimulus is promoting more bone formation in both the loaded and control limbs in group C than for any other group.

Figure 8: Mechanical Properties Suggest a Systemic Effect - The group loaded ten days after surgery (C48) is stiffer ($p=0.036$ versus group A and $p=0.004$ versus group D) and had a higher torque at failure ($p=0.024$ versus group A, $p=0.059$ versus group B, and $p=0.001$ versus group D) than any other group. The stiffness and ultimate failure torque are also higher in the control gaps of group C than in group D ($*p<0.05$). This suggests that the applied stimulus is promoting a more stiff and stronger structure in both the loaded and control limbs in group C than for any other group.

Figure 9: GFP Positive Cells in the Marrow - GFP positive cells were found in the marrow 48 days after surgery. At all of the time points there was evidence of some GFP positive staining, but it was not until day 48 that there were large populations of GFP positive cells in the marrow spaces. Cells were also present in other locations (cortices and pin sites), but the most consistent location for the MSC populations was in the medullary marrow (top) and the marrow within the periosteal callus (bottom).

Figure 10: Cells produce an adverse effect as measured by micro-CT and mechanical testing in torsion - The group that was stimulated on day 24 but did not have exogenous cells introduced had a higher bone volume, represented above by BMD ($p=0.011$), than the group that had cells injected via the tail vein on day 24. The same decreases due to cell injection were seen in the stiffness of the callus in torsion ($p=0.0301$, data not shown) and the torque to failure ($p=0.0142$).

Group	Displacement Initiation Day (Post-op)	Euthanasia Day 10: Group Name (μCT, histology, torsion)	Euthanasia Day 24: Group Name (μCT, histology, torsion)	Euthanasia Day 48: Group Name (μCT, histology, torsion)
A	0	A10 (n=11, 5, 5)	A24 (n=12, 3, 7)	A48 (n=8, 4, 4)
B	3	B10 (n=11, 5, 5)	B24 (n=11, 4, 5)	B48 (n=10, 3, 7)
C	10	--------	C24 (n=12, 5, 7)	C48 (n=11, 3, 5)
D	24	--------	--------	D48 (n=13, 5, 8)

Table 1: Nomenclature and Expermiental Group Sizes - This table shows the nomenclature for each group used in the study. The letters correspond to the timing of mechanical stimulation, and the numbers correspond to the day of euthanasia. The numbers in parentheses show the number of animals that were entered into the study for micro-CT, histology, and torsion testing.

Group	Marrow: Cell Score for Stimulated Limb	Marrow: Cell Score for Control Limb
A10	0.22	0.29
A24	0.52	0.50
A48	0.87	0.62
B10	0.13	0.11
B24	0.90	0.70
B48	1.38	1.04
C24	0.88	0.57
C48	0.67	0.42
D48	1.58	1.43

Table 2: Amount of MSCs in the Marrow Spaces - The scores for the amount of MSCs in the marrow spaces of the displaced and control limbs for each group show the stimulated limbs have more cellular activity in the marrow when compared to the unstimulated control limbs. The number of cells also increases with the amount of time after injection (i.e. A48>A24>A10), except in group C, which had cell delivery and axial displacement begin ten days after surgery.

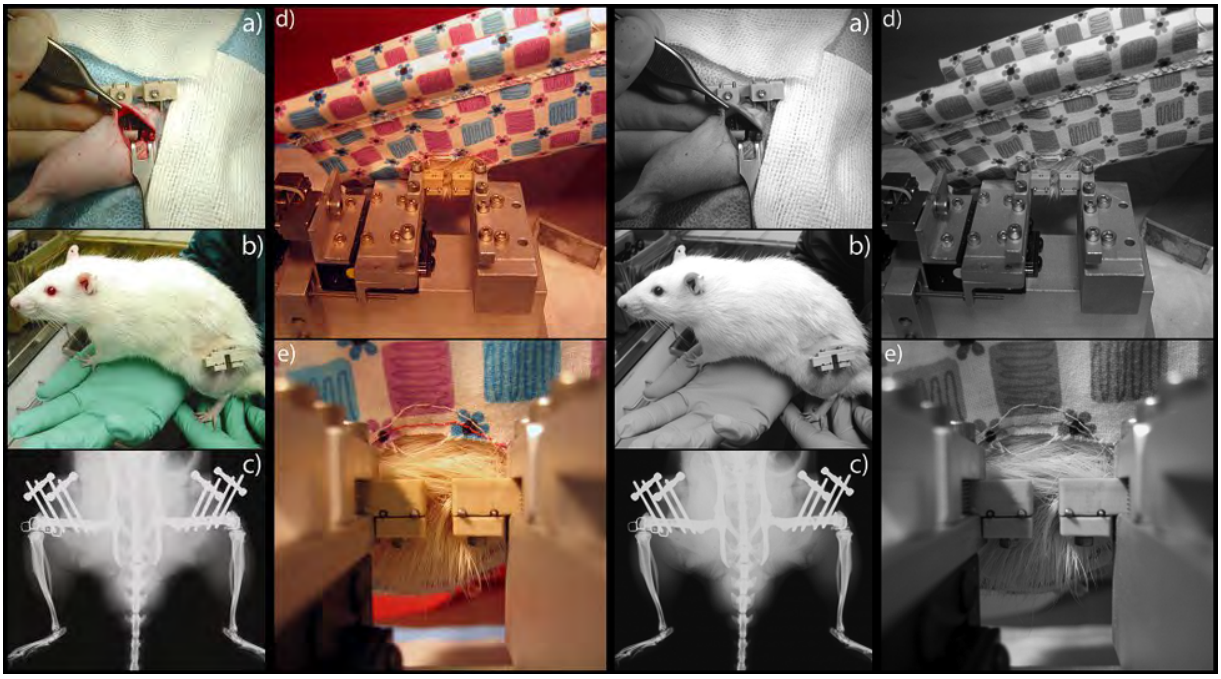

Figure 1: Overview of Surgery and Fixture for Axial Displacement - A two-millimeter segmental osteotomy was made at the mid-diaphysis of each femur (a). The fractures were stabilized using four threaded pins and a two-piece fixator that is locked in a rigid configuration for normal ambulation (b, c). During axial stimulation, the rat was anesthetized, placed in a sling, and the fixator was aligned with the fixture clamp (d). The close-up view of the fixator shows the two unlocked halves during stimulation (e).

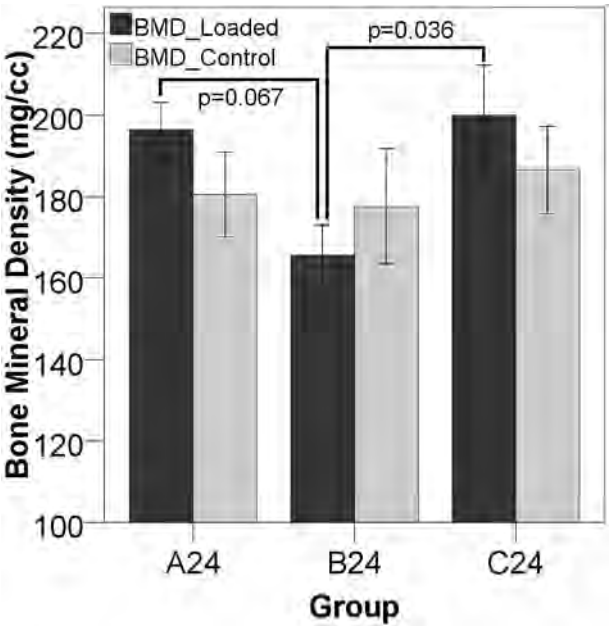

Figure 2: BMD 24 Days After Surgery - 24 days after surgery, fractures stimulated at three days post-op (B24) have reduced BMD compared to to those displaced immediately after (A24) or ten days after surgery (C24) suggesting that mechanical stimulation during the inflammatory stage of healing leads to a subsequent reduction in callus mineralization.

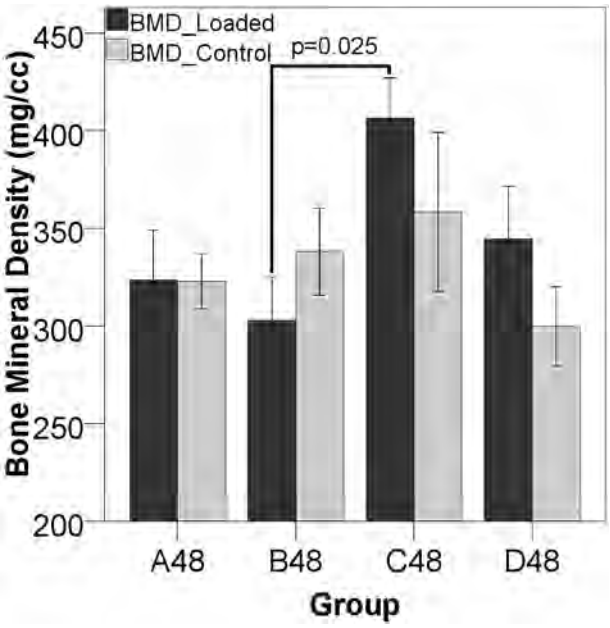

Figure 3: BMD 24 Days After Surgery - BMD is significantly higher in Group C (displacement beginning ten days post-op) versus Group B (displacement beginning three days post-op) 48 days after surgery. In the later stages of healing, the mineral content is higher on the displaced side in the animals loaded ten days post-operatively than those at other stimulation time points. This reached a significant increase over the defects displaced three days post-op, since the mineral levels in those gaps were slightly depressed compared to the other groups.

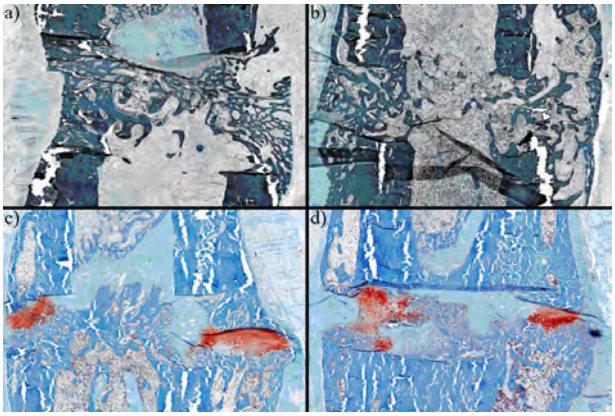

Figure 4: Histology for the Group Stimulated Ten Days After Surgery (Group C48) - When the axial displacement is started ten days after surgery, the stimulated limbs have no cartilage and have bony bridging by day 48 (shown above). The unstimulated controls have a substantial amount of bone, but still contain distinct areas of cartilage (in red). The figure shows: (a) a central section of a stimulated gap, (b) a peripheral section of a stimulated gap, (c) a central section of a control gap, and (d) a peripheral section of a control gap. Note that the difference in color between the top and the bottom images are an artifact of the staining procedure.

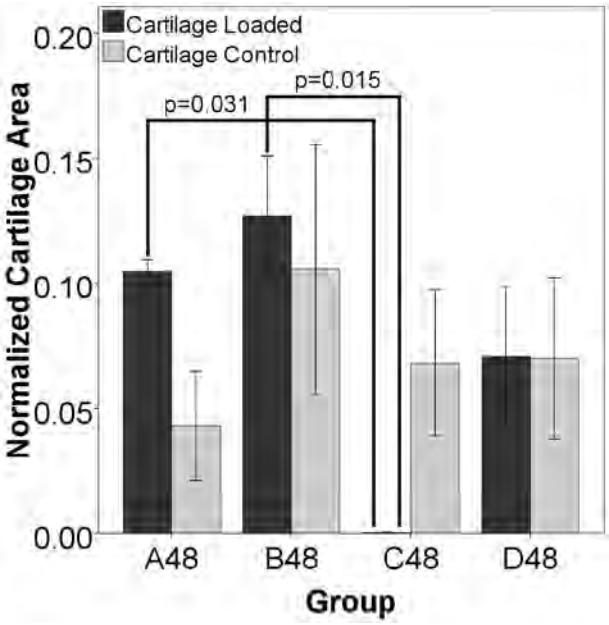

Figure 5: Cartilage area in animals euthanized 48 days post surgery - After 48 days, there is cartilage remaining in all groups, both stimulated and control, except for the gaps stimulated ten days after surgery (group C48). In these defects there is almost no cartilage remaining. The differences were significant between the displaced limbs of A48 and B48 in comparison to C48. There is also a significant difference between the displaced and contralateral control in group C48 ($p=0.045$, sig not shown), with the displaced side containing significantly less cartilage than the control. There is also more cartilage in the displaced side in group A48 when compared to the contralateral control ($p=0.037$, sig not shown).

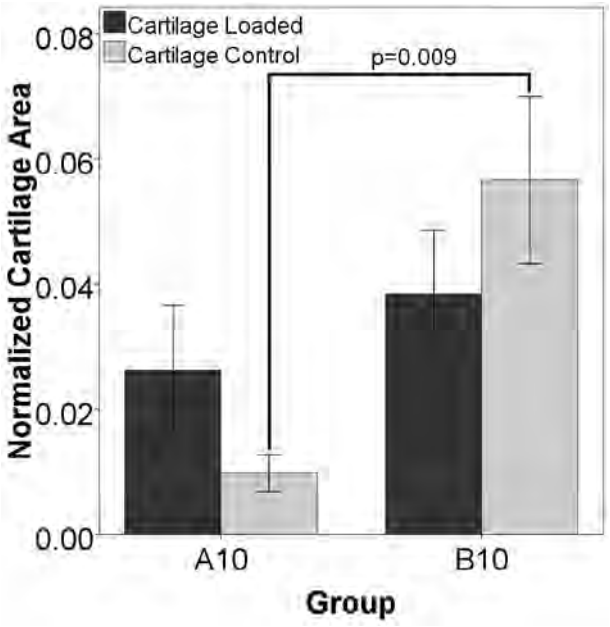

Figure 6: Histology Suggests a Systemic Effect - Histology shows differences between control limbs at day ten, suggesting a systemic effect. For animals euthanized ten days after surgery, there is an overall increase in cartilage area (stimulated and control combined) in the group stimulated three days after surgery (group B10) when compared to defects from animals stimulated immediately after surgery (group A10) (p=0.002). The control gaps from these animals also display an increased amount of cartilage (shown above), suggesting that there may be a systemic effect due to load.

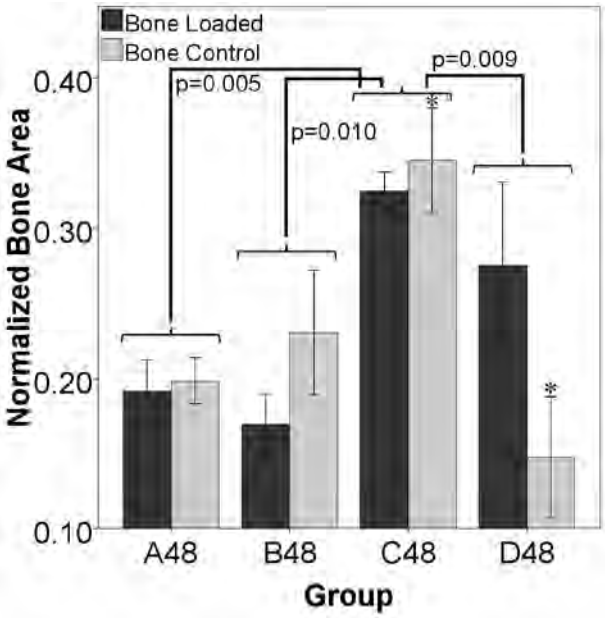

Figure 7: Bone Formation Suggests a Systemic Effect - Histology shows differences in normalized bone area from animals euthanized on day 48. The group loaded ten days after surgery (C48) has a higher percentage of bone as a whole (stimulated and control limbs considered together) than any other group (p=0.005 with group A, p=0.010 with group B, and p=0.009 with group D). There is also more bone in the control gap of C48 than in the control gap of D48 (*p=0.011). These results suggest that the applied stimulus is promoting more bone formation in both the loaded and control limbs in group C than for any other group.

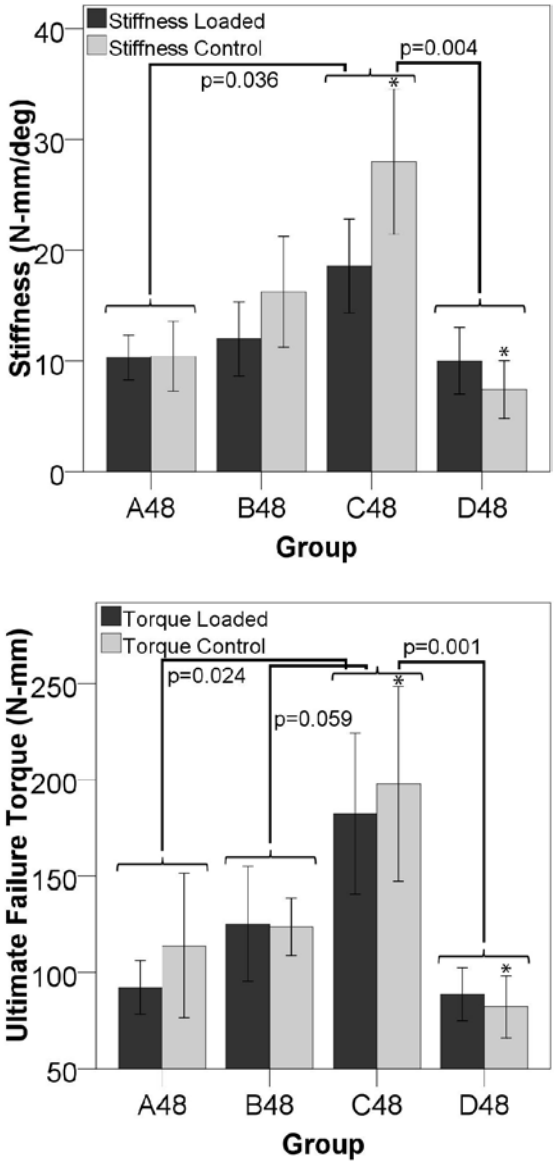

Figure 8: Mechanical Properties Suggest a Systemic Effect - The group loaded ten days after surgery (C48) is stiffer (p=0.036 versus group A and p=0.004 versus group D) and had a higher torque at failure (p=0.024 versus group A, p=0.059 versus group B, and p=0.001 versus group D) than any other group. The stiffness and ultimate failure torque are also higher in the control gaps of group C than in group D (*p<0.05). This suggests that the applied stimulus is promoting a more stiff and stronger structure in both the loaded and control limbs in group C than for any other group.

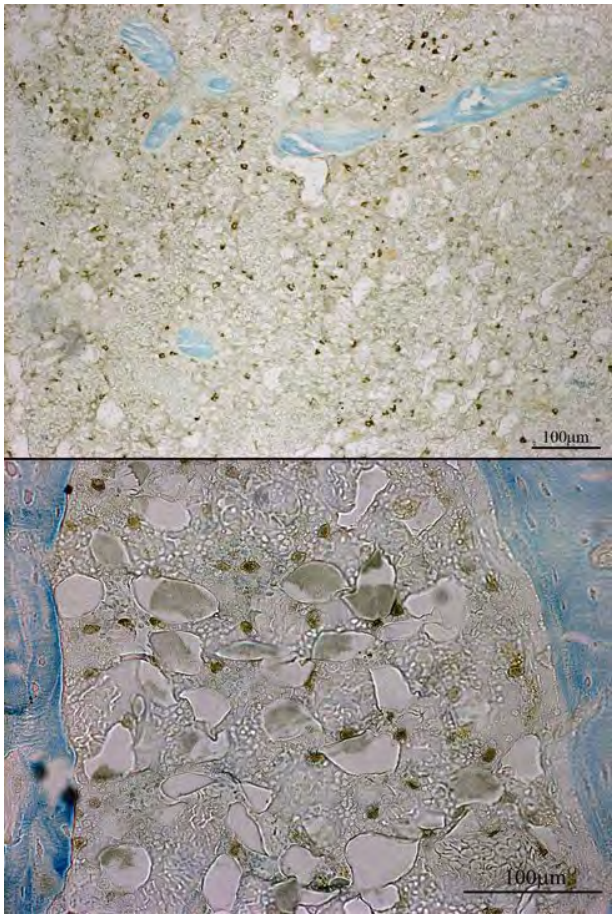

Figure 9: GFP Positive Cells in the Marrow - GFP positive cells were found in the marrow 48 days after surgery. At all of the time points there was evidence of some GFP positive staining, but it was not until day 48 that there were large populations of GFP positive cells in the marrow spaces. Cells were also present in other locations (cortices and pin sites), but the most consistent location for the MSC populations was in the medullary marrow (top) and the marrow within the periosteal callus (bottom).

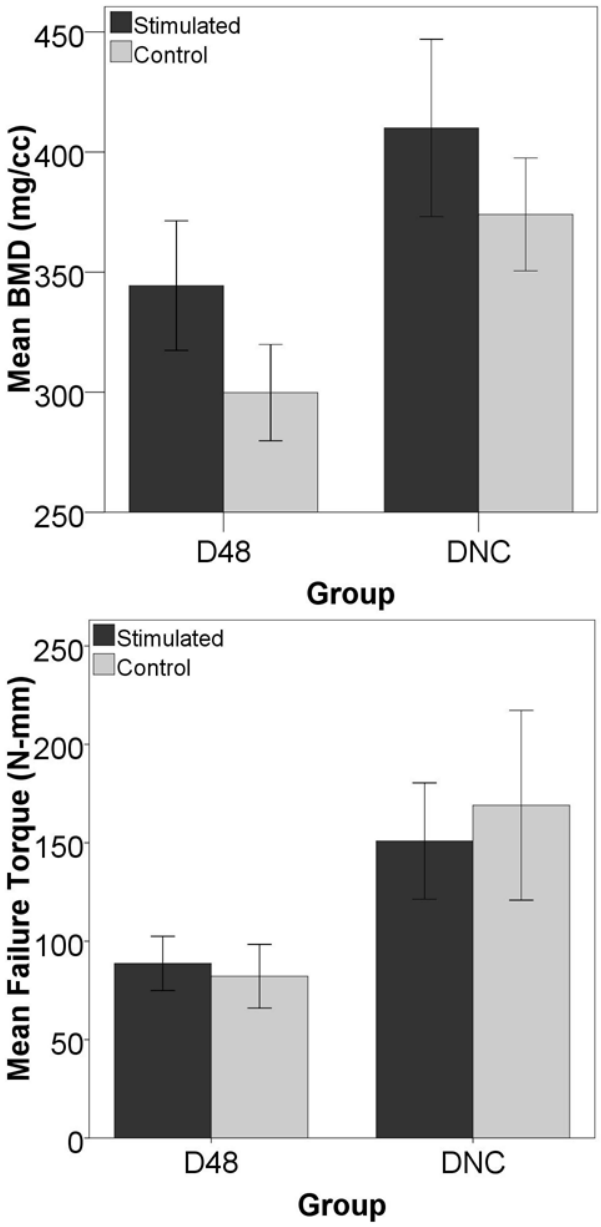

Figure 10: Cells produce an adverse effect as measured by micro-CT and mechanical testing in torsion - The group that was stimulated on day 24 but did not have exogenous cells introduced had a higher bone volume, represented above by BMD (p=0.011), than the group that had cells injected via the tail vein on day 24. The same decreases due to cell injection were seen in the stiffness of the callus in torsion (p=0.0301, data not shown) and the torque to failure (p=0.0142).